Proteomic interactome of *C. elegans* Mediator complex subunit 28 (MDT-28) reveals predominant association with a restricted set of core Mediator subunits and an affinity to additional structural and enzymatic proteins

Petr Yilma[1], Markéta Kostrouchová[1,2], Pavel Talacko[3], Veronika Kostrouchová[1], David Kostrouch[1], Petr Novák[4] and Marta Kostrouchová[1]

1 Biocev, First Faculty of Medicine, Charles University, Průmyslová 595, 252 42 Vestec, Czech Republic

2 Department of Pathology, Third Faculty of Medicine, Charles University, Ruská 87, 10000 Praha 10, Czech Republic

3 Laboratory of Mass Spectrometry, Faculty of Science, Charles University, Průmyslová 595, 252 42 Vestec, Prague, Czech Republic

4 Biocev, Laboratory of Structural Biology and Cell Signaling, Institute of Microbiology of the Czech Academy of Sciences, Prague, Vídeňská 1083, 142 20, Czech Republic

*Corresponding author:

Marta Kostrouchová

Biocev, First Faculty of Medicine,

Charles University,

Průmyslová 595, 252 50 Vestec,

Czech Republic

email: marta.kostrouchova@lf1.cuni.cz

Abstract

Transcription factors exert their regulatory potential on RNA Polymerase II machinery through a multiprotein complex called Mediator complex or Mediator. The Mediator complex integrates regulatory signals from cell regulatory cascades with the regulation by transcription factors. The Mediator complex consists of 25 subunits in *Saccharomyces cerevisiae* and 30 or more subunits in multicellular eukaryotes. Mediator subunit 28 (MED28), along with MED30, MED23, MED25 and MED26 belong to presumably evolutionarily new subunits that seem to be absent in unicellular eukaryotes and are likely to have evolved together with multicellularity and cell differentiation. Previously, we have shown that an originally uncharacterized predicted gene F28F8.5 is the true MED28 orthologue in *Caenorhabditis elegans* (MDT-28) and showed that it is involved in a spectrum of developmental processes. Here, we studied the proteomic interactome of MDT-28 edited as GFP::MDT-28 using Crispr/Cas9 technology or MDT-28::GFP expressed from extrachromosomal arrays in transgenic *C. elegans* exploiting the GFP-TRAP system and mass spectrometry. The results show that MDT-28 associates with the Head module subunits MDT-6, MDT-8, MDT-11, MDT-17, MDT-20, MDT-22 and MDT-30 and the Middle module subunit MDT-14. The analyses also identified additional proteins as preferential MDT-28 interactants including chromatin organizing proteins, structural proteins and enzymes. The results provide evidence for MDT-28 engagement in the Mediator Head Module and support the possibility of physical (direct or indirect) interaction of MDT-28 with additional proteins, reflecting a

transcription-regulating potential of primarily structural and enzymatic proteins at the level of the Mediator complex.

Introduction

The Mediator complex, also called Mediator, is a large multiprotein complex that connects regulation by transcription factors (TFs) with the basal transcription machinery. This complex serves as a hub for integration of diverse regulatory signals such as kinase cascades with the regulation of gene expression (Asturias et al. 1999; Allen and Taatjes 2015; Soutourina 2018). Mediator can be divided into four structural modules, Middle module, Head module, Tail Module and Kinase module and this modular arrangement can be recognized from yeast to mammals (Bourbon 2008; Jiang et al. 1998; Dotson et al. 2000; Tsai et al. 2014; Harper and Taatjes 2017). The Mediator complex in *Saccharomyces cerevisiae* contains fewer subunits than its mammalian or plant equivalents (Soutourina 2018). Four subunits seem to be specific for multicellular organisms and are absent in *S. cerevisiae*: MED23, MED25, MED26, MED28. Structural studies revealed the relative position of most core Mediator subunits (Asturias et al. 1999; Dotson et al. 2000; Mathur et al. 2011; Robinson et al. 2012; Robinson et al. 2015; Robinson et al. 2016; Verger et al. 2019) but also several distinct steric conformations of Mediator dependent on its interaction with specific transcription factors (SREBP, VP16, TR, VDR of p53AD) (Poss et al. 2013). The exact position of MED28 and MED30 is still not sufficiently elucidated (Soutourina 2018).

The Mediator complex exists in two main forms, a larger complex containing probably most or all subunits of all four modules and a smaller complex lacking the Kinase module. Mediator that is missing the Kinase module is often linked to the formation of a more transcriptionally active Mediator. Some subunits have paralogs whose incorporation into Mediator have subspecialization functions for transcription regulation (Allen and Taatjes 2015). Beside that, the existence of complexes lacking one or

more subunits was reported in yeast which yield strains viable under laboratory conditions despite the lack of some subunits. While Med 17 and Med 21 were indispensable for wide transcription (Holstege et al. 1998; Thompson and Young 1995), others including Med1, Med2, Med3, Med5, Med9, Med15, Med16, Med18, Med19, Med20, Med31, and CDK module subunits Med12 (srb8), Med13 (srb9), srb10 (CDK8), and srb11 were found non-essential as single mutants could have been maintained under laboratory conditions (Dettmann et al. 2010). Although under special conditions (in Yeast (Robinson et al. 2016) and in HeLa cells (Paoletti et al. 2006; Tsai et al. 2014)) most subunits were found in equimolar ratios, suggesting a fixed number of main Mediator subunits, some subunits immunoprecipitated at higher amounts (Paoletti et al. 2006). In tumors, numerous studies report upregulation or downregulation of individual subunits with links to biological behavior of cancer cells (Bragelmann et al. 2016; Syring et al. 2016).

MED28 has a special position in-between Mediator subunit proteins for its early discovered dual regulatory role, one as a Mediator subunit (Sato et al. 2004; Beyer et al. 2007) and the second, which is cytoplasmic, at the level of the cytoskeleton (Gonzalez-Agosti et al. 1996; Wiederhold et al. 2004; Lee et al. 2006; Lu et al. 2006; Huang et al. 2012).

In this study we explored the protein interactome of *C. elegans* MDT-28 using its edited form GFP::MDT-28 or a transgenic form MDT-28::GFP and the GFP-TRAP system. The data show predominant association of MDT-28 with core Mediator subunits and support the engagement of MDT-28 in Head module of Mediator complex.

Materials and Methods

Strains and transgenic lines

Two *Caenorhabditis elegans* lines expressing MDT-28 tagged with GFP were used:

1. The KV4 (8419) line with edited F28F8.5 in the form *gfp*::F28F8.5 in its normal genomic position $P_{F28F8.5}$(V:15573749)::*gfp*::*F28F8.5* on both alleles (Kostrouchova et al. 2017) expressing edited GFP::MDT-28.

2. The *C. elegans* line 7949 with $P_{F28F8.5(400\ bp)}$::*F28F8.5*::*gfp* carrying extrachromosomal arrays with a construct containing the 400 bp internal promoter of *F28F8.5*, the genomic sequence of F28F8.5 fused with the sequence coding for GFP with artificial introns (amplified from the pPD95.75 vector together with the 3′ UTR originally from the *unc-54*) and the pRF4 selection marker (Kostrouchova et al. 2017).

For controls, a *C. elegans* line carrying extrachromosomal arrays with the promoter of *nhr-180* regulating the expression of *gfp* alone (Kostrouchova et al. 2018) was used (Fig.1).

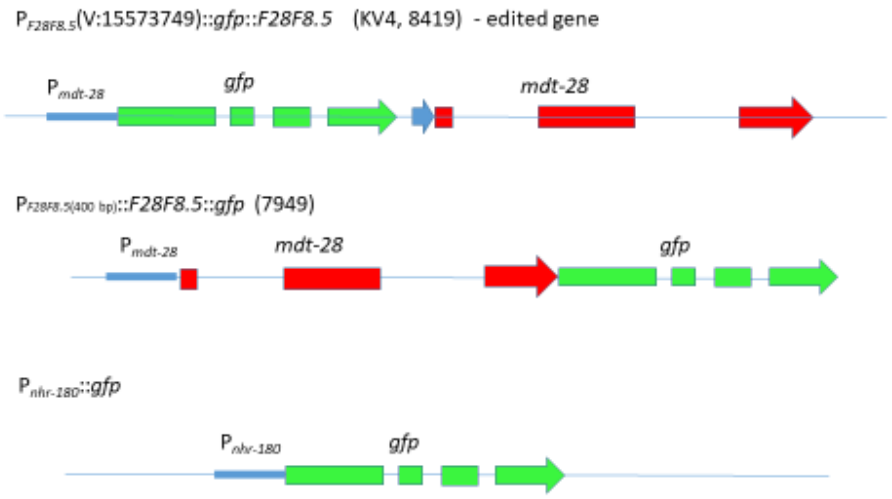

Fig. 1. Schematic representation the edited alleles and constructs used in this study.

Laboratory cultures for large-scale nematode preparations

For immunoprecipitation experiments the *C. elegans* lines were cultured on Petri dishes (diameter 60 mm) containing Nematode Growth Medium agar covered with OP50 *E. coli* as described (Brenner 1974). *C. elegans* cultures were incubated in an air-conditioned laboratory with dim illumination (tempered to 22.5° C) until the cultures reached visually similar population density and contained similar representation of individual larval stages, adults and laid embryos; this was reached usually in 4 days. The mixed stages nematodes were controlled for the expression of GFP tagged MDT-28 in the line 7949 and showed the tendency to gradually lose GFP tagged MDT-28

and was therefore checked for the proportion of nematodes positive for GFP fluorescence. Only cultures with more than 60% of GFP-positive animals were used for further experiments. The nematodes were washed with deionized water, pelleted by centrifugation in 12 ml tubes (1400 rpm, in Hettich Universal 32 R centrifuge, r_{max} = 120 mm, approximate maximal centrifugal force 176 xg, 4° C, 2 minutes) (Hettich states 150 xg at this conditions in the swing-out rotor). Nematodes were resuspended in deionized water and pelleted to final samples that were stored at -80 ° C until further processing.

GFP-TRAP pull-down experiments

The GFP-Trap system available from Chromotek (https://www.chromotek.com/products/nano-traps/gfp-trap/) was used for pull-down of GFP-tagged MDT-28 and of GFP alone used as control as described (Kostrouchova et al. 2018) with modifications regarding the scale of individual precipitations and amount of lysate from mixed cultures of nematodes. Briefly, the *C. elegans* line 8419 with *mdt-28* gene edited in the form $P_{F28F8.5}$(V:15573749)::*gfp*::*F28F8.5* on both alleles (Kostrouchova et al. 2017), the transgenic line carrying extrachromosomal arrays $P_{F28F8.5}$ (400 bp)::*F28F8.5*::*gfp* and the control line carrying extrachromosomal arrays containg $P_{nhr-180}$(1361bp)::*gfp* were cultured on agar Petri dishes. The expression of GFP alone or GFP tagged proteins was checked under Olympus SZX12 microscope (Olympus, Tokyo, Japan). The mixed stages nematodes were washed with Dilution-Wash Buffer (50 mM HEPES pH7.4, 1 mM EGTA, 1mM MgCl2, 100 mM KCl). The nematodes were pelleted by centrifugation in ice-cold lysis buffer (50 mM HEPES pH7.4, 1 mM EGTA, 1mM MgCl2, 100 mM KCl, 10 % glycerol (v/v), 0.5% NP-40 (v/v)); all purchased from Sigma-Aldrich (St. Louis, Mo, USA). The maximum obtainable amount of packed nematodes (raging from 1 to 2.6 ml) were used for each individual

GFP-Trap preparation. Samples were resuspended in an equal volume of lysis buffer with protease and phosphatase inhibitors (Halt™ Protease and Phosphatase Inhibitor Cocktail (100x), Thermo Fisher Scientific, Waltham, MA, USA) to obtain a final 1x solution of inhibitors. Nematodes were sonicated 10 times 15 s (with 45 s pauses) on ice (UP50H Ultrasonic Processor, Hielscher Ultrasound Technology, Teltow, Germany). Aliquots were controlled for complete lysis under the microscope. The samples were centrifuged for 25 min at 18600 x g and 4° C. The supernatant was transferred to a pre-cooled tube and 500 µl of Dilution - Wash buffer supplemented with 1x Protease inhibitors was added. GFP-TRAP magnetic beads (***GFP***-Trap®_MA); purchased from ChromoTek, Planegg-Martinsried, Germany) were prepared according to the manufacturer's recommendations. Fifty microliters of bead slurry was resuspended in 500 µl of ice-cold dilution buffer, the beads were pulled-down using the magnetic separator and this step was repeated two more times. The diluted lysate was mixed with the equilibrated beads and the cleared supernatant was incubated at 4° C for 12 hrs. Beads with bound proteins were pulled-down using the magnetic separator and washed three times using Dilution - Wash buffer.

Elution

Proteins bound to the beads were eluted by 50 µl 0,2M Glycine (pH 2,5) during 30 s under constant mixing followed by magnetic separation. The supernatant was transferred to a new tube and 5 ul 1M Tris base (pH 10.4) was used for sample neutralization. The remaining beads were stored in wash buffer and also analyzed by Mass Spectrometry.

Mass spectrometry

For mass spectrometry, the eluates and in some cases also the remaining beads were acetone precipitated and resuspended in 100mM Triethylammonium bicarbonate (TEAB) containing 1% sodium

deoxycholate (SDC). Cysteines were reduced with 5mM (final) tris(2-carboxyethyl)phosphine (TCEP) (60 °C, 60 min.) and blocked with 10 mM (final) methyl methanethiosulfonate (MMTS) (all Thermo Fisher Scientific) (10 min., 22 °C).

Proteins were cleaved with 1µg of trypsin at 37°C overnight, centrifuged, supernatants collected and acidified with TFA (1% final concentration). SDC was removed by extraction with ethyl acetate. Peptides were desalted on the Peptide Optitrap column (Optimize Technologies, Oregon City, U.S.A.). Nano Reversed phase column (EASY-Spray column, 50 cm x 75 µm ID, PepMap C18, 2 µm particles, 100 Å pore size) (Thermo Fisher Scientific, Waltham, MA) was used for LC/MS/MS analysis. The mobile phase buffers were: A - water and 0.1% formic acid, B - acetonitrile and 0.1% formic acid. The samples were loaded onto the trap column (Acclaim PepMap300, C18, 5 µm, 300 Å Wide Pore, 300 µm x 5 mm, 5 Cartridges) for 4 min at 15 µl/min. The loading buffer was composed of water, 2% acetonitrile and 0.1% trifluoroacetic acid. Peptides were eluted with the Mobile Phase B gradient from 4% to 35% B in 60 min. Eluted peptide cations were converted to gas-phase ions by electrospray ionization and analyzed on a Thermo Orbitrap Fusion (Q-OT- qIT, Thermo Fisher Scientific, Waltham, MA). Survey scans of peptide precursors from 400 to 1600 m/z were performed at 120K resolution (at 200 m/z) with a 5×10^5 ion count target. Tandem MS was performed by isolation at 1.5 Th with the quadrupole, HCD fragmentation (higher-energy collisional dissociation) with normalized collision energy of 30, and rapid scan MS analysis in the ion trap. The MS 2 ion count target was set to 10^4 and the max injection time was 35 ms. Only those precursors with charge states 2–6 were sampled for MS 2. The dynamic exclusion duration was set to 45 s with a 10 ppm tolerance around the selected precursor and its isotopes. Monoisotopic precursor selection was turned on. The instrument was run in top speed mode with 2 s cycles. All data were analyzed and quantified with the MaxQuant software (version 1.5.3.8) (Cox et al. 2014). The false discovery rate (FDR)

was set to 1% for both proteins and peptides and a minimum length of seven amino acids. The Andromeda search engine was used for the MS/MS spectra search against the *C. elegans* database (downloaded from Uniprot on April 2015, containing 25 527 entries) and further updates. Enzyme specificity was set as C-terminal to Arg and Lys, also allowing cleavage at proline bonds and a maximum of two missed cleavages. Dithiomethylation of cysteine was selected as fixed modification and N-terminal protein acetylation and methionine oxidation as variable modifications. The "match between runs" feature of MaxQuant was used to transfer identifications to other LC-MS/MS runs based on their masses and retention time (maximum deviation 0.7 min) and used in quantification experiments. Quantifications were performed with the label-free algorithms and data analysis was performed using the Perseus 1.5.2.4 software (Masuda et al. 2008; Cox et al. 2014; Hebert et al. 2014; Tyanova et al. 2016).

The raw data were deposited to an open database https://www.ebi.ac.uk/pride/archive/ with the accession number PXD015552 (**Project DOI:** 10.6019/PXD015552, **Username:** reviewer73133@ebi.ac.uk, **Password:** 2l2cgHCZ). The raw data concerning relevant proteins are also provided in four Excel files that list raw data analyzed by Perseus program (http://coxdocs.org/doku.php?id=perseus:start version Perseus_1.6.1.3) and are accessible at Folia Biologica Website as Supplementary data:

20180226_Yilma_C1_E1,E6.ods

20180504_Yilma_C2_E2.ods

20180829_Yilma_C3_E3,E4.ods

20190224_Yilma_C4_E5.ods

The experiments are marked as in Table 1 and Table 2: C1 to C4 are the control samples and E1 to E6 are experimental samples.

Results

Identification of Mediator complex subunits associating with MDT-28 from mixed stages *C. elegans* cultures

For the detection of proteins preferentially interacting with MDT-28 *in vivo*, two *C. elegans* strains expressing MDT-28 tagged by GFP and a commercially available system GFP-Trap for isolating GFP tagged proteins, were used. Four control experiments were performed in order to exclude proteins binding non-specifically to GFP or the beads containing the anti-GFP single chain antibody. Proteins identified in extracts prepared from animals expressing MDT-28 tagged with GFP on their N- or C-terminus were compared with controls. As a positive result for protein detection, the intensity threshold of 18 and identification of at least 2 peptides was set as the criteria for reliable identification. For the classification of a detected protein as an MDT-28 interactor, only proteins falling under the threshold and classified as undetected by Perseus program in all four control experiments but identified in lysates from lines with tagged MDT-28 were taken into account.

Prominently, a set of proteins classified as Mediator subunits was identified as MDT-28 interactants (Table 1). They included mostly subunits of the Head module: MDT-6, MDT-8, MDT-11, MDT-17, MDT-20, MDT-22 and MDT-30. The set of MDT-28 interactants further included MDT-14 of the Middle module. The other Middle module subunits, Tail module subunits or Kinase module subunits were not identified in our screens as MDT-28 interactants under the experimental conditions and given selection criteria. MDT-18 was identified in two out of four experiments, however this identification is statistically less significant since it is based only on one unique peptide.

Table 1. Mediator complex subunits identified in MDT-28 pull-down experimetns

	Ctrl 1	Ctrl 2	Ctrl 3	Ctrl 4	Exp 1	Exp 2	Exp 3	Exp 4	Exp 5	Exp 6
	GFP	GFP	GFP	GFP	C-term (7949)	C-term (7949)	C-term (7949)	N-term (8419)	N-term (8419)	N-term (8419)
MDT-6	-	-	-	-	+	-	-	-	+	+
MDT-8	-	-	-	-	+	-	-	+	+	+
MDT-11	-	-	-	-	+	-	-	+	+	+
MDT-14	-	-	-	-	-	-	-	+	+	+
MDT-17	-	-	-	-	+	+	+	+	+	+
MDT-20	-	-	-	-	-	-	-	-	+	+
MDT-22	-	-	-	-	-	-	-	+	+	-
MDT-28	-	-	-	-	+	+	+	+	+	-
MDT-30	-	-	-	-	+	-	-	+	+	+

Legend to Table 1. Detection of predicted Mediator subunits in immunoprecipitated samples from control experiments (marked as Ctrl 1 to 4) based on *C. elegans* expressing GFP alone, C-terminally tagged MDT-28::GFP expressed from extrachromosomal arrays (marked as Exp 1 to 3 in yellow table cells) and N-terminally tagged GFP::MDT-28 expressed from *C. elegans* line with edited *mdt-28* (marked as Exp 4 to 6 in green table cells). While control experiments did not show presence of any known Mediator subunit, lines with GFP-tagged MDT-28 contained interacting Mediator complex subunits.

MDT-28 associates with additional structural and enzymatic proteins

Comparison of the data from all experiments yielded a relatively small number of proteins that could have been classified as MDT-28 interactants under the chosen selection criteria (Table 1). The set of MDT-28 interacting proteins included proteins falling under the category of proteins likely to be involved in the regulation of transcription or other nuclear events and proteins that are not classified as primarily transcription regulating proteins. Some identified MDT-28 interactants belong to the category of structural or enzymatic proteins or proteins with contemporary unknown

functions (Table 2). This set of potential MDT-28 interactants includes chromatin organizing proteins, known nuclear transporters, nucleolar proteins and enzymes. Two proteins classified as RPL proteins were identified as strong binders, RPL-24.2 and RPL-29, in immunoprecipitated samples.

Additionally, a set of mitochondrial ribosomal proteins of the small subunit was detected as potential interactants of MDT-28. This set included MRPS-2, MRPS-5, MRPS-6, MRPS-7, MRPS-15 and MRPS-26. The set of proteins immunoprecipitated with MDT-28 also included components of the Ubiquinol-cytochrome C oxidoreductase complex (UCR-1.1, UCR-2.1, UCR-2.2 and UCR-2.3) and UCR-11, which is also predicted to be a component of this complex.

Table 2. Additional MDT-28 interactants

	Ctrl 1	Ctrl 2	Ctrl 3	Ctrl 4	**Exp 1**	**Exp 2**	**Exp 3**	**Exp 4**	**Exp 5**	**Exp 6**	**GO/ notes**
	GFP	GFP	GFP	GFP	C- (7949)	C- (7949)	C- (7949)	N- (8419)	N- (8419)	N- (8419)	
ARX-1		-	-	-	-	+	+	+	+	-	**Actin binding**
DHC-1	-	-	-	-	-	-	-	+	+	-	**Enzyme Cytoskeleton**
EKL-4	-	-	-	-	-	-	+	+	-	-	**Corepressor**
GLY-7	-	-	-	-	-	+	+	+	+	-	**N/C enzyme Golgi**
HECD-1	-	-	-	-	-	+	-	-	+	-	**E3 ligase Nuclear**
HRP-2	-	-	-	-	+	-	+	-	+	+	**Ribonucleo-protein**
IMA-3	-	-	-	-	-	+	+	-	+	-	**Nuclear import signal receptor activity**
LET-716	-	-	-	-	-	+	+	+	+	-	**Nucleic acid binding**
NGP-1 GNL2 homol.	-	-	-	-	-	+	+	+	+	-	**Enzyme GTPase, NMD**
RPL-24.2	-	-	-	-	+	+	+	+	+	-	
RPL-29	-	-	-	-	+	+	+	+	+	+	
SWAN-1	-	-	-	-	-	+	+	+	+	-	**N/C enzyme GTPase**
VBH-1	-	-	-	-	+	+	+	-	+	+	**Helicase**

Legend to Table 2. Detection of MDT-28 interactants in immunoprecipitated samples from control experiments (marked as Ctrl 1 to 4) based on *C. elegans* expressing GFP alone, C-terminally tagged MDT-28::GFP expressed from extrachromosomal arrays (marked as Exp 1 to

3 in yellow table cells) and N-terminally tagged GFP::MDT-28 expressed from *C. elegans* line with edited *mdt-28* (marked as Exp 4 to 6 in green table cells). GO – gene ontology related to possible nuclear and cytoplasmic functions.

Discussion

MDT-28 has tight interactions with selected Mediator Head subunits and Middle Module subunit MDT-14 (and Middle Module subunit MDT-9 in some experiments)

Our experiments show that MDT-28 associates with a set of core Mediator complex subunits consisting mainly of Head module subunits and Middle module subunit MDT-14. MDT-28 is a small protein comprising of only 200 or 202 amino acids and it is therefore likely that the identified proteins are extracted from the cellular material as a protein complex or multiple versions of smaller complexes. Our results further support the classification of MDT-28 as the orthologue of MED28 which is known to form contacts with the Head module subunits in proteomic studies (Tsai et al. 2014). Our results thus support the classification of MDT-28 and MED28 orthologues as a Head module subunit. The interactions of two subunits, MDT-30 and MDT-6, were reported earlier based on *in vitro* methods. The interaction with MDT-30 is likely to be direct since it was observed earlier on isolated proteins made in bacteria (Kostrouchova et al. 2017). The results support the prediction of MDT-30 as an MED30 orthologue. In contrary to other orthologues of Mediator subunits in *C. elegans* that have a similar size as yeast and vertebrate counterparts, MDT-30 is substantially bigger than its mammalian orthologues. MDT-30 contains 466 amino acids compared to human and mouse MED30 which contain only 143 and 178 amino acids, respectively. The Clustal analysis indicates relatively high degree of conservation of the C-

terminal half of MDT-30 with almost entire sequence of human MED30 (isoform 1) (E Value 6 e-04, 26.83% identity over the conserved region spanning 218 amino acids and 3 gaps for the total of 8 amino acids). While the conserved region has globular character in both nematode and human proteins, the N-terminal region present in nematode MED30 orthologue has a character of intrinsically disordered protein.

A superposition of Mediator subunits identified as MDT-28 preferential interactants suggests the possibility of a complex that may be prevalent in lysates obtained from mixed stages *C. elegans*. The starting material that was used in our experiments is likely to contain a large proportion of tissues forming the majority of *C. elegans* bodies, such as gut, muscles and gonads.

It can be expected that the binding proteins may differ for N-terminally and C-terminally tagged MDT-28 for two reasons; first due to sterical blocking of interacting domains of MDT-28, and secondly because of the relatively larger cytoplasmic expression of C-terminally tagged MDT-28 expressed from extrachromosomal arrays.

The C-terminal globular domain of MDT-28 is likely to be important for interactions with other Mediator subunits. The N-terminal IDR is likely to mediate interactions with multiple proteins and assume its actual conformation during MED-28 assembly in the protein complex. The two variants of GFP tagged MDT-28 are also expressed differently. The edited N-terminally tagged protein is expressed ubiquitously in a pattern that is likely to represent the natural expression of untagged MDT-28 including expression in gonads while the C-terminally tagged MDT-28 is expressed strongly in the cytoplasm and in the nuclei of gut and epidermal cells but not in gonads, where the expression from extrachromosomal arrays is silenced. Nevertheless, the interaction with Mediator subunits was detected in both arrangements.

Since the Mediator subunits immunoprecipitated with MDT-28 are more likely to be precipitated in our experiments as a protein complex rather than proteins associated with MDT-28 individually, the immunoprecipitated complex is likely to represent a core MDT-28 containing Mediator complex (Fig. 2). Although some components of the MDT-28 containing Mediator complex may be removed from the complex during purification steps, the remaining complex is likely to reflect the most resistant and thus preferential protein complex that contains MDT-28.

Fig. 2. Schematic representation of MDT-28 core Mediator

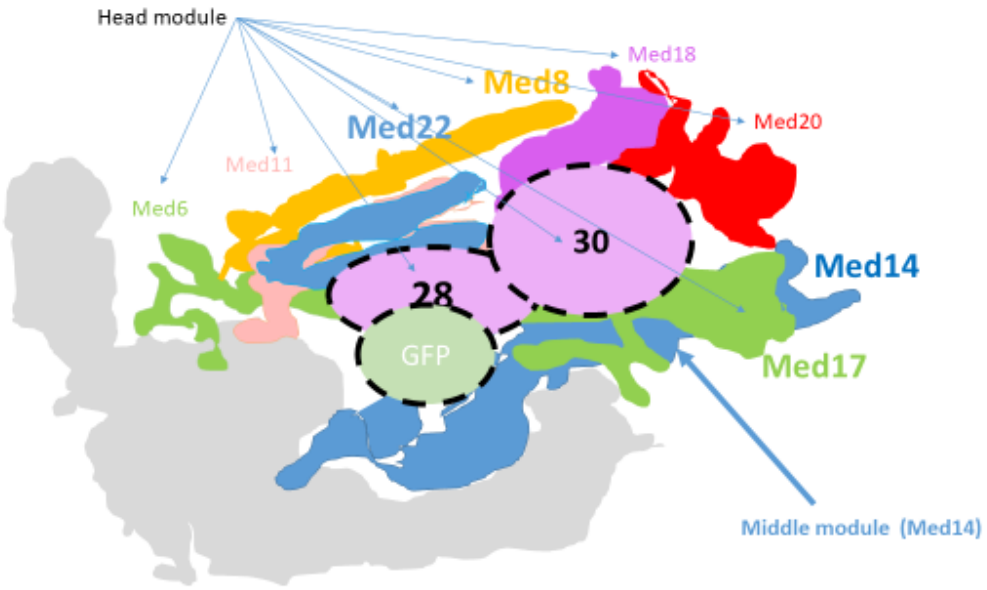

Fig. 2 A hypothetical MDT-28 containing core Mediator based on the known structure of yeast core Mediator (Nozawa et al. 2017) and Mediator subunits immunoprecipitated with MDT-28. The domains occupied by individual proteins are indicated with colors corresponding to indicated Mediator subunits. MDT-28 tagged by GFP and MDT-30 are positioned arbitrarily to the central region of the yeast Mediator complex that is less densely filled by Mediator subunits in the core Mediator complex determined by Nozava et al. (Nozawa et al. 2017).

Nuclear and cytoplasmic proteins of diverse nature interact with MDT-28

While the validity of the Mediator complex subunits that were identified as MDT-28 interactors is supported by numerous proteomic and functional studies, the possibility of functional relevance of additional MDT-28 interactors is supported only indirectly. Since MDT-28 as well as MED28 are both nuclear and cytoplasmic proteins (Wiederhold et al. 2004; Lee et al. 2006; Kostrouchova et al. 2017; Kostrouchova et al. 2018) they are likely to interact with proteins mediating their actual subcellular localization in both main cellular compartments.

Our screens were performed at relatively very stringent conditions that were necessary for disintegration of nematodes prior to the immunoprecipitation steps. This is keeping with the fact that only a part of the core Mediator subunits were immunoprecipitated with MDT-28. This also gives presumption that possible cytoplasmic proteins identified in our screens may be directly involved in protein interactions at the cytoskeleton that is well documented but the proteins directly binding MED28 to the cytoskeleton are not known (Wiederhold et al. 2004).

A candidate protein identified in our screens that can mediate interaction with actin cytoskeleton is ARX-1, the orthologue of human ACTR3 (Actin-related protein 3), which is a constituent of the Arp2/3 complex. This complex is located at the cell surface and regulates cell shape and motility together with F-actin and Cortactin (Weed et al. 2000). ARP2/3 is also localized in nuclei and has a known function in the regulation of actin polymerization linked to gene expression and DNA break clustering in homology-directed DNA repair (Schrank et al. 2018), an event that involves the presence of the Mediator complex (Soutourina and Werner 2014).

Another primarily cytoplasmic protein that was identified in our screens as an MDT-28 interactor is dynein heavy chain DHC-1. It was identified in two out of three experiments exploiting N-terminally tagged MDT-28 with high intensities and 22 identified unique peptides. Dynein is involved in numerous protein interactions both in the cytoplasm and in the nucleus. It has been shown to interact with P53 protein and the glucocorticoid receptor (Harrell et al. 2004)

Additional MDT-28 interactors including EKL-4, GLY-7, HECD-1, HRP-2, IMA-3, LET-716, NGP-1, VBH-1, DHC-1, RPL-24.2 and RPL-29 may also be functionally relevant since their nuclear and often transcription regulating functions are listed in molecular biology databases. The two proteins classified as ribosomal proteins, RPL-24.2 and RPL-29 are not classical ribosomal proteins, but are related based on sequence similarity. Both RPL-29 and RPL-24.2 may have transcription regulation functions. RPL-29 is homologous to HIP/RPL29 that was shown to be present in the cytoplasm as well as in the nucleus and to play more than one role during adult mammary gland development (Kirn-Safran et al. 2002). RPL-24.2 is an orthologue of RSL24D1 which has a known primary nuclear localization but at the present with unknown function (The Human Protein Atlas, https://www.proteinatlas.org/ENSG00000137876-RSL24D1/cell).

Our experiments identified a set of mitochondrial ribosomal proteins of the small ribosomal subunit as likely interactants with MDT-28 or MDT-28 containing Mediator complex. This subset was identified in experiments exploiting both forms of the MDT-28 GFP tagged protein. It seems more likely that these proteins form a protein complex rather than being bound individually since small subunit components are represented more than other mitochondrial ribosomal proteins. It is a question, if the identified proteins are kept together by another protein or something else, e.g. mitochondrial rRNA or other molecules of similar nature. It is unlikely that the complex would

be in fact a complete small mitochondrial ribosomal subunit since other proteins of the complete small mitochondrial ribosomal subunit are missing in our screens. It is possible that mitochondrial ribosomal proteins were interacting with the immunoprecipitated MDT-28 during our experimental procedures at steps of cell disintegration. The observed situation may, however, reflect a physiologically relevant process, the mitochondrial stress response (Hill et al. 2018). The interaction of mitochondrial ribosomal proteins with proteins central to the regulation of transcription may have functional consequences that is supported by the concept of regulation of plant development by ribosomal proteins (Robles and Quesada 2017). It may be compatible with the proposed concept of "The Ribosome Filter Redux" or "The ribosome filter hypothesis" (Mauro and Edelman 2002; Mauro and Edelman 2007).

Funding sources: This work was supported by the European Regional Development Fund "BIOCEV — Biotechnology and Biomedicine Centre of the Academy of Sciences and Charles University in Vestec" (CZ.1.05/1.1.00/02.0109) (The Start-Up Grant to the group Structure and Function of Cells in Their Normal State and in Pathology – Integrative Biology and Pathology (5.1.10)) and the LQ1604 National Sustainability Program II (Project BIOCEV-FAR) from the Ministry of Education, Youth and Sports of Czech Republic; The grants PROGRES Q26/LF1 and PROGRES Q28/LF1 and LF3 "Oncology" from Charles University; The grant SVV 260 377 from the Charles University, Czech Republic. This work was supported by the project OPPK No. CZ.2.16/3.1.00/24024, awarded by European Fund for Regional Development (Prague & EU – We invest for your future). The funders had no role in study design, data collection and analysis, decision to publish, or preparation of the manuscript.

Acknowledgements. Authors thank Dr. Zdeněk Kostrouch for advice.

References

Allen, B. L., Taatjes, D. J. (2015) The Mediator complex: a central integrator of transcription. *Nat Rev Mol Cell Biol* 16:155-166.

Asturias, F. J., Jiang, Y. W., Myers, L. C., Gustafsson, C. M., Kornberg, R. D. (1999) Conserved structures of mediator and RNA polymerase II holoenzyme. *Science* 283:985-987.

Beyer, K. S., Beauchamp, R. L., Lee, M. F., Gusella, J. F., Naar, A. M., Ramesh, V. (2007) Mediator subunit MED28 (Magicin) is a repressor of smooth muscle cell differentiation. *J Biol Chem* 282:32152-32157.

Bourbon, H. M. (2008) Comparative genomics supports a deep evolutionary origin for the large, four-module transcriptional mediator complex. *Nucleic Acids Res* 36:3993-4008. 10.1093/nar/gkn349

Bragelmann, J., Klumper, N., Offermann, A., von Massenhausen, A., Bohm, D., Deng, M., Queisser, A., Sanders, C., Syring, I., Merseburger, A. S., Vogel, W., Sievers, E., Vlasic, I., Carlsson, J., Andren, O., Brossart, P., Duensing, S., Svensson, M. A., Shaikhibrahim, Z., Kirfel, J., Perner, S. (2016) Pan-Cancer Analysis of the Mediator Complex Transcriptome Identifies CDK19 and CDK8 as Therapeutic Targets in Advanced Prostate Cancer. *Clin Cancer Res*. 10.1158/1078-0432.CCR-16-0094

Brenner, S. (1974) The genetics of Caenorhabditis elegans. *Genetics* 77:71-94.

Cox, J., Hein, M. Y., Luber, C. A., Paron, I., Nagaraj, N., Mann, M. (2014) Accurate proteome-wide label-free quantification by delayed normalization and maximal peptide ratio extraction, termed MaxLFQ. *Mol Cell Proteomics* 13:2513-2526. 10.1074/mcp.M113.031591

Dettmann, A., Jaschke, Y., Triebel, I., Bogs, J., Schroder, I., Schuller, H.-J. (2010) Mediator subunits and histone methyltransferase Set2 contribute to Ino2-dependent transcriptional activation of phospholipid biosynthesis in the yeast Saccharomyces cerevisiae. *Molecular genetics and genomics : MGG* 283:211-221.

Dotson, M. R., Yuan, C. X., Roeder, R. G., Myers, L. C., Gustafsson, C. M., Jiang, Y. W., Li, Y., Kornberg, R. D., Asturias, F. J. (2000) Structural organization of yeast and mammalian mediator complexes. *Proc Natl Acad Sci U S A* 97:14307-14310. 10.1073/pnas.260489497

Gonzalez-Agosti, C., Xu, L., Pinney, D., Beauchamp, R., Hobbs, W., Gusella, J., Ramesh, V. (1996) The merlin tumor suppressor localizes preferentially in membrane ruffles. *Oncogene* 13:1239-1247.

Harper, T. M., Taatjes, D. J. (2017) The complex structure and function of Mediator. *J Biol Chem*. 10.1074/jbc.R117.794438

Harrell, J. M., Murphy, P. J., Morishima, Y., Chen, H., Mansfield, J. F., Galigniana, M. D., Pratt, W. B. (2004) Evidence for glucocorticoid receptor transport on microtubules by dynein. *J Biol Chem* 279:54647-54654. 10.1074/jbc.M406863200

Hebert, A. S., Richards, A. L., Bailey, D. J., Ulbrich, A., Coughlin, E. E., Westphall, M. S., Coon, J. J. (2014) The one hour yeast proteome. *Mol Cell Proteomics* 13:339-347. 10.1074/mcp.M113.034769

Hill, S., Sataranatarajan, K., Remmen, H. V. (2018) Role of Signaling Molecules in Mitochondrial Stress Response. *Front Genet* 9:225. 10.3389/fgene.2018.00225

Holstege, F. C., Jennings, E. G., Wyrick, J. J., Lee, T. I., Hengartner, C. J., Green, M. R., Golub, T. R., Lander, E. S., Young, R. A. (1998) Dissecting the regulatory circuitry of a eukaryotic genome. *Cell* 95:717-728.

Huang, C. Y., Chou, Y. H., Hsieh, N. T., Chen, H. H., Lee, M. F. (2012) MED28 regulates MEK1-dependent cellular migration in human breast cancer cells. *J Cell Physiol* 227:3820-3827. 10.1002/jcp.24093

Jiang, Y. W., Veschambre, P., Erdjument-Bromage, H., Tempst, P., Conaway, J. W., Conaway, R. C., Kornberg, R. D. (1998) Mammalian mediator of transcriptional regulation and its possible role as an end-point of signal transduction pathways. *Proc Natl Acad Sci U S A* 95:8538-8543.

Kirn-Safran, C. B., Julian, J., Fongemie, J. E., Hoke, D. E., Czymmek, K. J., Carson, D. D. (2002) Changes in the cytologic distribution of heparin/heparan sulfate interacting protein/ribosomal protein L29 (HIP/RPL29) during in vivo and in vitro mouse mammary epithelial cell expression and differentiation. *Dev Dyn* 223:70-84. 10.1002/dvdy.1226

Kostrouchova, M., Kostrouch, D., Chughtai, A. A., Kassak, F., Novotny, J. P., Kostrouchova, V., Benda, A., Krause, M. W., Saudek, V., Kostrouchova, M., Kostrouch, Z. (2017) The nematode homologue of Mediator complex subunit 28, F28F8.5, is a critical regulator of C. elegans development. *PeerJ* 5:e3390. 10.7717/peerj.3390

Kostrouchova, M., Kostrouchova, V., Yilma, P., Benda, A., Mandys, V., Kostrouchova, M. (2018) Valproic Acid Decreases the Nuclear Localization of MDT-28, the Nematode Orthologue of MED28. *Folia Biol (Praha)* 64:1-9.

Lee, M. F., Beauchamp, R. L., Beyer, K. S., Gusella, J. F., Ramesh, V. (2006) Magicin associates with the Src-family kinases and is phosphorylated upon CD3 stimulation. *Biochem Biophys Res Commun* 348:826-831. 10.1016/j.bbrc.2006.07.126

Lu, M., Zhang, L., Sartippour, M. R., Norris, A. J., Brooks, M. N. (2006) EG-1 interacts with c-Src and activates its signaling pathway. *Int J Oncol* 29:1013-1018.

Masuda, T., Tomita, M., Ishihama, Y. (2008) Phase transfer surfactant-aided trypsin digestion for membrane proteome analysis. *J Proteome Res* 7:731-740. 10.1021/pr700658q

Mathur, S., Vyas, S., Kapoor, S., Tyagi, A. K. (2011) The Mediator complex in plants: structure, phylogeny, and expression profiling of representative genes in a dicot (Arabidopsis) and a monocot (rice) during reproduction and abiotic stress. *Plant Physiol* 157:1609-1627. 10.1104/pp.111.188300

Mauro, V. P., Edelman, G. M. (2002) The ribosome filter hypothesis. *Proc Natl Acad Sci U S A* 99:12031-12036. 10.1073/pnas.192442499

Mauro, V. P., Edelman, G. M. (2007) The ribosome filter redux. *Cell Cycle* 6:2246-2251. 10.4161/cc.6.18.4739

Nozawa, K., Schneider, T. R., Cramer, P. (2017) Core Mediator structure at 3.4 A extends model of transcription initiation complex. *Nature* 545:248-251. 10.1038/nature22328

Paoletti, A. C., Parmely, T. J., Tomomori-Sato, C., Sato, S., Zhu, D., Conaway, R. C., Conaway, J. W., Florens, L., Washburn, M. P. (2006) Quantitative proteomic analysis of distinct

mammalian Mediator complexes using normalized spectral abundance factors. *Proc Natl Acad Sci U S A* 103:18928-18933. 10.1073/pnas.0606379103
Poss, Z. C., Ebmeier, C. C., Taatjes, D. J. (2013) The Mediator complex and transcription regulation. *Crit Rev Biochem Mol Biol* 48:575-608. 10.3109/10409238.2013.840259
Robinson, P. J., Bushnell, D. A., Trnka, M. J., Burlingame, A. L., Kornberg, R. D. (2012) Structure of the mediator head module bound to the carboxy-terminal domain of RNA polymerase II. *Proc Natl Acad Sci U S A* 109:17931-17935. 10.1073/pnas.1215241109
Robinson, P. J., Trnka, M. J., Bushnell, D. A., Davis, R. E., Mattei, P. J., Burlingame, A. L., Kornberg, R. D. (2016) Structure of a Complete Mediator-RNA Polymerase II Pre-Initiation Complex. *Cell* 166:1411-1422 e1416. 10.1016/j.cell.2016.08.050
Robinson, P. J., Trnka, M. J., Pellarin, R., Greenberg, C. H., Bushnell, D. A., Davis, R., Burlingame, A. L., Sali, A., Kornberg, R. D. (2015) Molecular architecture of the yeast Mediator complex. *Elife* 4. 10.7554/eLife.08719
Robles, P., Quesada, V. (2017) Emerging Roles of Mitochondrial Ribosomal Proteins in Plant Development. *Int J Mol Sci* 18. 10.3390/ijms18122595
Sato, S., Tomomori-Sato, C., Parmely, T. J., Florens, L., Zybailov, B., Swanson, S. K., Banks, C. A., Jin, J., Cai, Y., Washburn, M. P., Conaway, J. W., Conaway, R. C. (2004) A set of consensus mammalian mediator subunits identified by multidimensional protein identification technology. *Mol Cell* 14:685-691.
Schrank, B. R., Aparicio, T., Li, Y., Chang, W., Chait, B. T., Gundersen, G. G., Gottesman, M. E., Gautier, J. (2018) Nuclear ARP2/3 drives DNA break clustering for homology-directed repair. *Nature* 559:61-66. 10.1038/s41586-018-0237-5
Soutourina, J. (2018) Transcription regulation by the Mediator complex. *Nat Rev Mol Cell Biol* 19:262-274. 10.1038/nrm.2017.115
Soutourina, J., Werner, M. (2014) A novel link of Mediator with DNA repair. *Cell Cycle* 13:1362-1363. 10.4161/cc.28749
Syring, I., Klumper, N., Offermann, A., Braun, M., Deng, M., Boehm, D., Queisser, A., von Massenhausen, A., Bragelmann, J., Vogel, W., Schmidt, D., Majores, M., Schindler, A., Kristiansen, G., Muller, S. C., Ellinger, J., Shaikhibrahim, Z., Perner, S. (2016) Comprehensive analysis of the transcriptional profile of the Mediator complex across human cancer types. *Oncotarget* 7:23043-23055. 10.18632/oncotarget.8469
Thompson, C. M., Young, R. A. (1995) General requirement for RNA polymerase II holoenzymes in vivo. *Proc Natl Acad Sci U S A* 92:4587-4590.
Tsai, K. L., Tomomori-Sato, C., Sato, S., Conaway, R. C., Conaway, J. W., Asturias, F. J. (2014) Subunit architecture and functional modular rearrangements of the transcriptional mediator complex. *Cell* 157:1430-1444. 10.1016/j.cell.2014.05.015
Tyanova, S., Temu, T., Sinitcyn, P., Carlson, A., Hein, M. Y., Geiger, T., Mann, M., Cox, J. (2016) The Perseus computational platform for comprehensive analysis of (prote)omics data. *Nat Methods* 13:731-740. 10.1038/nmeth.3901
Verger, A., Monte, D., Villeret, V. (2019) Twenty years of Mediator complex structural studies. *Biochem Soc Trans*. 10.1042/BST20180608
Weed, S. A., Karginov, A. V., Schafer, D. A., Weaver, A. M., Kinley, A. W., Cooper, J. A., Parsons, J. T. (2000) Cortactin localization to sites of actin assembly in lamellipodia requires interactions with F-actin and the Arp2/3 complex. *J Cell Biol* 151:29-40. 10.1083/jcb.151.1.29

Wiederhold, T., Lee, M. F., James, M., Neujahr, R., Smith, N., Murthy, A., Hartwig, J., Gusella, J. F., Ramesh, V. (2004) Magicin, a novel cytoskeletal protein associates with the NF2 tumor suppressor merlin and Grb2. *Oncogene* 23:8815-8825.

Original Article

Valproic Acid Decreases the Nuclear Localization of MDT-28, the Nematode Orthologue of MED28

(Mediator complex / valproic acid / nuclear localization / MDT-28 / MED28)

M. KOSTROUCHOVÁ[1,2,*], V. KOSTROUCHOVÁ[1], P. YILMA[1], A. BENDA[3], V. MANDYS[2], M. KOSTROUCHOVÁ[1,‡]

[1]Biocev, First Faculty of Medicine, Charles University, Prague, Czech Republic
[2]Department of Pathology, Third Faculty of Medicine, Charles University, Prague, Czech Republic
[3]Imaging Methods Core Facility, Biocev, Faculty of Science, Charles University, Prague, Czech Republic

Abstract. Mediator is a multiprotein complex that connects regulation mediated by transcription factors with RNA polymerase II transcriptional machinery and integrates signals from the cell regulatory cascades with gene expression. One of the Mediator subunits, Mediator complex subunit 28 (MED28), has a dual nuclear and cytoplasmic localization and function. In the nucleus, MED28 functions as part of Mediator and in the cytoplasm, it interacts with cytoskeletal proteins and is part of the regulatory cascades including that of Grb2. MED28 thus has the potential to bring cytoplasmic regulatory interactions towards the centre of gene expression regulation. In this study, we identified MDT-28, the nematode orthologue of MED28, as a likely target of lysine acetylation using bioinformatic prediction of post-translational modifications. Lysine acetylation was experimentally confirmed using anti-acetyl lysine antibody on immunoprecipitated GFP::MDT-28 expressed in synchronized *C. elegans*. Valproic acid (VPA), a known inhibitor of lysine deacetylases, enhanced the lysine acetylation of GFP::MDT-28. At the subcellular level, VPA decreased the nuclear localization of GFP::MDT-28 detected by fluorescence-lifetime imaging microscopy (FLIM). This indicates that the nuclear pool of MDT-28 is regulated by a mechanism sensitive to VPA and provides an indirect support for a variable relative proportion of MED28 orthologues with other Mediator subunits.

Received March 8, 2018. Accepted April 17, 2018.

This work was supported by the European Regional Development Fund "BIOCEV – Biotechnology and Biomedicine Centre of the Academy of Sciences and Charles University in Vestec" (CZ.1.05/1.1.00/02.0109) and the LQ1604 National Sustainability Program II (Project BIOCEV-FAR) and the project Biocev (CZ.1.05/1.1.00/02.0109) from the Ministry of Education, Youth and Sports of the Czech Republic; PROGRES Q26/LF1 and PROGRES Q28 "Oncology" from Charles University in Prague; grant SVV 260377/2017 from Charles University in Prague. The imaging was done at the Imaging Methods Core Facility at Biocev, Faculty of Science, Charles University, supported by the Czech-BioImaging large RI project (LM2015062 funded by MEYS CR). AB acknowledges the support by the MEYS CR (CZ.02.1.01/ 0.0/0.0/16 013/0001775 Czech-Bioimaging).

*Corresponding author: Markéta Kostrouchová, Biocev, First Faculty of Medicine, Charles University, Prague, Průmyslová 595, 252 42 Vestec, Czech Republic. Phone: (+420) 325 873 017; e-mail: marketa.kostrouchova@lf1.cuni.cz

Abbreviations: FLIM – fluorescence-lifetime imaging microscopy, MDT-28 – *C. elegans* orthologue of MED28, MED28 – Mediator complex subunit 28, NGM – nematode growth medium, PAIL – prediction of acetylation on internal lysines, RT – room temperature, TFs – transcription factors, VPA – valproic acid.

Introduction

Cell- and tissue-specific regulation of gene expression depends on transcription factors (TFs) (Reinke et al., 2013) and transcription cofactors that are expressed in a cell- and tissue-specific way (e.g. as exemplified on the mineralocorticoid receptor-dependent gene expression (Fuller et al., 2017)). TFs interact with RNA polymerase II (Pol II) basal transcriptional machinery through interaction with a multiprotein complex called Mediator complex or Mediator (Poss et al., 2013; Grants et al., 2015).

The overall structure of the Mediator complex can be divided into four modules named head, middle, tail, and the CDK8 module (Yin and Wang, 2014). Displacement of the CDK8 module forms a more transcriptionally active Mediator (Tsai et al., 2013).

The modules of Mediator consist of approximately 26 subunits in mammals, 29 subunits in *Caenorhabditis elegans* and 21 subunits in *Sacharomyces cerevisiae* (Allen and Taatjes, 2015; Grants et al., 2015). The subunit composition, arrangement and localization in the complex as well as the conformational shape of Mediator can be variable (Poss et al., 2013; Allen and Taatjes, 2015). Quantitative proteomic analysis identified under- or over-

representation of selected subunits in several human cell lines, yeast cultures and in numerous cancers (Kulak et al., 2014; Allen and Taatjes, 2015; Syring et al., 2016).

While orthologues of approximately 18 subunits can be identified both in yeast and Metazoa, some Mediator subunits are found only in yeast or only in higher metazoans. Mediator subunits that are found only in Metazoa include Med23, Med25, Med26, Med28, and Med30 (Harper and Taatjes, 2017). Mediator complex subunit 28 (MED28) is especially interesting because it not only has a nuclear, but also a cytoplasmic localization and function. In some cells and tissues MED28 is detected by specific antibodies predominantly in cytoplasmic territories, while in other cell types and tissue cultures it is detected predominantly in the nuclei, as can be seen from the data available in the Human Protein Atlas (https://www.proteinatlas.org/, access on January 23, 2018) (Uhlen et al., 2005, 2015, 2017; Thul et al., 2017). This protein was originally identified as a gene expressed in endothelial cells and named EG-1 (Endothelial-derived Gene-1) (Liu et al., 2002), but was later shown to be part of the Mediator complex and renamed MED28 (Sato et al., 2004; Beyer et al., 2007). MED28 (a.k.a. Magicin) also interacts with Growth factor receptor-bound protein 2 (Grb2) and Merlin and membrane-cytoskeleton scaffolding proteins at the plasma membrane (Wiederhold et al., 2004; McClatchey and Giovannini, 2005; McClatchey and Fehon, 2009) and was shown to associate with several Src-family kinases and to be their phosphorylation target (Lee et al., 2006). Overexpression of MED28 inhibits differentiation of smooth muscle cells in cell culture (Wiederhold et al., 2004).

In *C. elegans* the MED28 orthologue, MDT-28 (edited in the form expressing GFP/green fluorescent protein tagged at its N-terminus), also has a dual nuclear and cytoplasmic localization, suggesting that the capacity of transmitting cytoplasmic signals towards regulation of gene expression is evolutionarily conserved (Kostrouchova et al., 2017).

In this study we attempted to further characterize MDT-28. Bioinformatic analysis of the protein primary sequence of MDT-28 indicated that MDT-28 as well as numerous other MED28 orthologues from various phyla are likely targets of lysine acetylation. This hypothesis was supported by a positive signal of immunoprecipitated GFP::MDT-28 expressed in *C. elegans* with CRISPR/Cas-9-edited *mdt-28* that was augmented by treatment with valproic acid (VPA), a known inhibitor of lysine deacetylases. At the subcellular level, VPA treatment decreases the nuclear localization of GFP::MDT-28. The results show that the nuclear localization of MDT-28 is regulated by a mechanism sensitive to VPA, most likely by acetylation of lysines present in MDT-28 itself or in nuclear proteins interacting with MDT-28.

Material and Methods

Bioinformatics and identification of lysine acetylation

For prediction of lysine acetylation, the online predictor for protein acetylation PAIL (prediction of acetylation on internal lysines) was used (available at http://pail.biocuckoo.org/online.php) with threshold accuracy set at 85.13 %, 87.97 % and 89.21 % for low, medium and high thresholds, respectively (Li et al., 2006). Sequences of experimentally proven MDT-28 or of predicted orthologues were retrieved from GenBank (https://www.ncbi.nlm.nih.gov/genbank/) (Benson et al., 2013, 2017) (Table 1).

Strains, transgenic lines and genome editing

The *C. elegans* strain KV4 was used in which the gene for MDT-28 (F28F8.5b) was modified to *gfp::mdt-28* in its normal genomic position ($P_{F28F8.5}$*(V:15573749)::gfp::mdt-28*) on both alleles. The expressed GFP::MDT-28 was used for pull-down and fluorescence microscopy experiments. For details see Kostrouchova et al. (2017). A strain expressing GFP only from extrachromosomal

Table 1. Predicted acetylation sites of MED28 orthologues

Species	ID	Position	Peptide	HAT	Score	Cutoff	Stringency
C. elegans	H9G301.1 mdt-28	198	EAHPNAG**K**HFTT***	CREBBP	1.548	1.348	M
T. spiralis	tr|E5RZQ1|E5RZQ1_TRISP	163	KLTCSDW**K**IALES**	CREBBP	1.355	1.348	M
W. bancrofti	EJW84794.1	160	LSDLGAE**K**NSQGFE*	CREBBP	1.851	1.785	H
D. melanogaster	Q9VBQ9.1	189	ISRQMPP**K*******	CREBBP	2.161	1.785	H
H. sapiens	Q9H204.1	176	ANIPAPL**K**PT*****	CREBBP	2.165	1.785	H
M. musculus	Q920D3.2	176	ANIPAPLKQT*****	CREBBP	2.532	1.785	H
T. rubripes	XP_003972471.1	178	NLPPAPL**K**PS*****	CREBBP	2.698	1.785	H
X. tropicalis	AAI55039.1 med28	167	ANIPAPM**K**PT*****	CREBBP	2.165	1.785	H
C. intestinalis	XP_002124297.1	141	GAGSQQM**K**K******	CREBBP	3.391	1.785	H
C. intestinalis	XP_002124297.1 28-like	142	AGSQQMK**K*******	CREBBP	3.048	1.785	H
T. adhaerens	XM_002117398.1	105	QQDLTKW**K**E******	CREBBP	2.992	1.785	H

arrays under the regulation of the promoter of *nhr-180* (nuclear hormone receptor 180) was used as control for GFP::MDT28 pull-down experiments.

Valproic acid (VPA) treatment

These experiments were done on either nematode growth medium (NGM) plates or in liquid cultures containing a final concentration of 0 or 1 mM or 5 mM valproate (valproic acid sodium salt, Sigma-Aldrich, St. Louis, MO). OP50 bacteria also containing valproate at a final concentration of 0 or 1 mM or 5 mM covered the entire area of the respective plates. Synchronization of animals of the *C. elegans* strain KV4 was done using the bleach method overnight. The next day the L1 larvae were incubated with one of the three concentrations of valproate for 4 h or 24 h at room temperature (RT, 22 °C).

For FLIM experiments, control and VPA-treated nematodes were then placed in a 10 µl drop of PBS 1x on a glass microscopic slide (Waldemar Knittel Glasbearbeitungs-GmbH, Braunschweig, Germany) containing a layer of 2% agarose, immobilized with 1 mM levamisole (Sigma-Aldrich) and covered with a cover glass of thickness 0.13–0.17 mm with a refraction index of 1.523 (Hirschmann Laborgeräte GmbH & Co, Eberstadt, Germany).

For GFP-Trap experiments, after incubation with or without valproate the nematodes were washed with water followed by PBS 1x from plates, rocked for 10 min at room temperature, and pelleted 2 times by centrifugation at 250 × *g* for 3 min at 4 °C in 13 ml tubes, then in Eppendorf tubes (2 min at 330 × *g*, 4 °C). The worm pellets were immediately resuspended in 320 µl of ice-cold lysis buffer (10 mM Tris/Cl pH 7.5, 150 mM NaCl, 0.5 mM EDTA, 0.5% NP-40) with added protease inhibitors (Halt Protease and Phosphatase Inhibitor Cocktail (100x), Thermo Fisher Scientific, Waltham, MA) and vortexed with interruptions on ice for 10 min, followed by sonication (3 × 10 s). The lysed samples were spun down by centrifugation at 19,000 × *g* for 5 min at 4 °C and the supernatant was stored at –80 °C before performing GFP-Trap experiments.

GFP-Trap and proteomic analysis of MDT-28 acetylation

GFP-Trap experiments were done using GFP-Trap® MA (ChromoTek Inc., Hauppauge, NY) according to manufacturer's instructions with modifications. Experiments were done at constant excess of active beads (10 µl of bead slurry) that were incubated with the same amount of one of the three types of lysed samples obtained from animals treated with vehicle (deionized sterile water) or 1 mM or 5 mM VPA for 1 h at 4 °C. Beads with bound GFP or GFP::MDT-28 were magnetically separated and washed three times with Dilution/Wash buffer (10 mM Tris/Cl pH 7.5, 150 mM NaCl, 0.5 mM EDTA). The purified beads were then resuspended in 70 µl of 2× Tris-glycin SDS sample buffer (Thermo Fisher Scientific) and 2 µl of β-mercaptoethanol. To dissociate immunocomplexes from the beads, 95 °C heat was applied for 10 min followed by centrifugation at around 13,000 × *g* for 5 min at RT, and samples were stored at 4 °C.

For Western blotting, 10 µl or 20 µl of each supernatant was loaded on two SDS-gels, separated by electrophoresis and then blotted onto two BioTrace™ PVDF transfer membranes using the Mini-PROTEAN Tetra Cell (Bio-Rad, Hercules, CA). Blocking was done in either 0.3 % (for detection of acetylated lysine) or 5 % (for detection of GFP) non-fat milk in T-PBS for 30 min at RT. Incubation with primary antibodies was done with shaking overnight at 4 °C. Primary antibodies used were mouse acetyl-lysine monoclonal antibody 1C6 (at a dilution of 1 : 1000) (Abcam, Cambridge, MA) and mouse GFP antibody B-2 (at a dilution of 1 : 222) (sc-9996, Santa Cruz Biotechnology, Santa Cruz, CA). Secondary antibody used was goat anti-mouse antibody (H+L)-HRP conjugate (1 : 10,000) (Bio-Rad).

Fluorescence-lifetime imaging microscopy (FLIM)

FLIM acquisition was done as described (Kostrouchova et al., 2017). Briefly, the single photon counting signal from the internal hybrid detectors in Leica TC SP8 SMD FLIM (Leica, Wetzlar, Germany), acquired during confocal acquisitions, was simultaneously processed by HydraHarp400 TCSPC electronics (PicoQuant, Berlin, Germany). General data structure, the demo program description and user instructions are accessible at https://github.com/PicoQuant/PicoQuant-Time-Tagged-File-Format-Demos/blob/master/PTU/Matlab/Read_PTU.m). We used our own implementation of TTTR data analysis, written in LabVIEW, which allows proper handling of the bidirectional harmonic scan with line accumulation and/or sequential excitation. The emission signal upon 488 nm excitation was spectrally split into two hybrid detectors with similar intensity at each of them to lower the detector saturation at bright pixels. The signal from both time synchronized channels was added up. The false colour scale (1 to 3 ns) is based on the average photon arrival time.

Densitometric analysis of FLIM images

FLIM data of the *C. elegans* KV4 strain were recorded at identical settings in one microscopic session and exported as false colour scale images in TIFF format in two assembled files for 4 h and 24 h incubation with or without VPA. Experiments after 4 h incubation included controls (exposed to vehicle only) and animals exposed to 1 mM or 5 mM VPA. Experiments after 24 h incubation included controls and animals treated with 1 mM VPA. To remove the contribution of autofluorescence from the quantification of overall densities, the GFP signal amplitude in each pixel was estimated from the average arrival time of photons in that pixel, assuming a two-component model consisting of GFP and the autofluorescence signal. The amplitude of the GFP signal was encoded as the red channel in the exported false

colour images. Exported TIFF images were analysed using the ImageJ program. The images were split to individual channels and all clearly defined intestinal nuclei in the red channel recordings were densitometrically analysed (using the rectangle selection tool). The rectangles were set as the minimum possible rectangles that could be drawn around the nuclei, touching the nuclei on four sides.

Results

Bioinformatic analyses of MED28 orthologues reveal a high probability of lysine acetylation

The 202 amino acid sequence of MDT-28/F28F8.5b (WormBase ID: WP:CE47319, www.wormbase.org/species/c_elegans/protein/WP:CE47319#06-10K) contains four lysines: K107, K120, K128 and K198. For the prediction of possible lysine acetylation we used the online bioinformatic tool PAIL (http://bdmpail.biocuckoo.org). Under medium stringency settings all four lysines in the primary amino acid sequence were identified as targets of acetylation. Under high stringency settings, lysines 128 and 198 were identified with a score of 1.20 and 2.13, respectively against a threshold of 0.5.

We then used the GPS-PAIL program (http://pail.biocuckoo.org/online.php) for the prediction of substrates and sites of seven histone acetyltransferases that identified K198 as the likely target of CREB-binding protein (CBP, CREBBP), also under medium stringency settings (with a score of 1.548 at 1.348 cutoff) (Table 1). The same prediction tool identified a high probability of lysine acetylation in all selected protein sequences of the known Mediator subunit 28 orthologues across the animal kingdom (Table 1).

The sequence analysis for targets of defined acetyltranferases (NP_079481.2) identified the most C-terminal lysine (K176) of human MED28 as the likely target of CBP-mediated acetylation (with the score of 2.165) (Table 1). In both the human MED28 and the *C. elegans* orthologue, the lysines recognized as the likely targets of CBP-dependent acetylation are the most C-terminal lysines located in the regions that are not classified by homology searches as conserved. These C-terminally positioned lysines are conserved within the metazoan classes. While in nematodes the lysines identified as CBP targets are the 5th, 6th or 7th amino acid from the C-terminal end in *C. elegans*, *T. spiralis* and *W. bancrofti*, respectively, in *Drosophila* it is the last C-terminal amino acid, in vertebrates it is the 3rd terminal amino acid, the second to last or last in *Ciona intestinalis*, and in the sequence retrieved from the *T. adhaerens* genome using the Blast program as the closest sequence to human MED28, there is a lysine recognized as a likely CBP target also in the second to last amino acid (Table 1). In several insect species, the prediction of acetylated lysines is not found in the most C-terminal part of predicted proteins, but several other lysines are identified as likely targets of acetylation under high stringency settings (e.g., in XP_011140830.1, the predicted mediator of RNA polymerase II transcription subunit 28 isoform X2 of *Harpegnathos saltator*). The prediction was also done using the GPS-PAIL computer program (http://pail.biocuckoo.org/online.php).

C. elegans GFP::MDT-28 is dynamically acetylated

To test whether or not MDT-28 is acetylated, we used the *C. elegans* strain KV4 expressing GFP::MDT-28 from both edited alleles containing the edited gene *gfp::mdt-28*. The GFP::MDT-28 fusion protein was immunoprecipitated using the GFP-Trap system (in excess of beads with single-chain anti-GFP antibody) from synchronized animals, and acetylated lysines were detected on Western blot using an anti-acetylated lysine monoclonal antibody. The anti-acetylated lysine antibody yielded a positive signal on the fusion protein but not on GFP alone, supporting the presence of acetylated lysines in MDT-28. The signal obtained with the anti-acetyl lysine antibody was considerably weaker compared to that obtained with the anti-GFP antibody. We therefore treated synchronized cultures of *C. elegans* larvae with VPA, a known inhibitor of histone deacetylases. In keeping with the prediction, VPA increased the signal detected by anti-lysine antibody more than the expression of GFP::MDT-28 detected by the anti-GFP antibody (Fig. 1).

Valproic acid decreases the intranuclear localization of GFP::MDT-28

To visualize GFP::MDT-28 localization we used FLIM, which is able to detect and resolve from the autofluorescence background the weak signal of GFP::MDT-28 expressed from its two edited alleles, and we compared the basal state of its expression with that after the treatment with 1 mM and 5 mM VPA. While under basal conditions GFP::MDT-28 was localized predominantly in the nuclei with a prominent dotted pattern, treatment with 1 mM and 5 mM VPA for 4 h decreased the gross nuclear expression of GFP::MDT-28 and its dotted character (Fig. 2). Densitometric analysis of the values exported in the red channel confirmed the overall decrease of GFP::MDT-28 nuclear presence in *C. elegans* incubated with 1 and 5 mM VPA (Fig. 3). This effect of VPA was even more apparent in animals treated with VPA for 24 h (Fig. 4). The strong FLIM signal visible in the nuclei in a dotted pattern decreased after 24 h treatment with 1 mM VPA. Densitometric analysis of the values exported in the red channel taken after 24 h also confirmed a strong decrease of GFP::MDT-28 intranuclear localization after the treatment with VPA (Fig. 5).

Discussion

While most Mediator complex subunits have characteristics of predominantly or exclusively nuclear proteins,

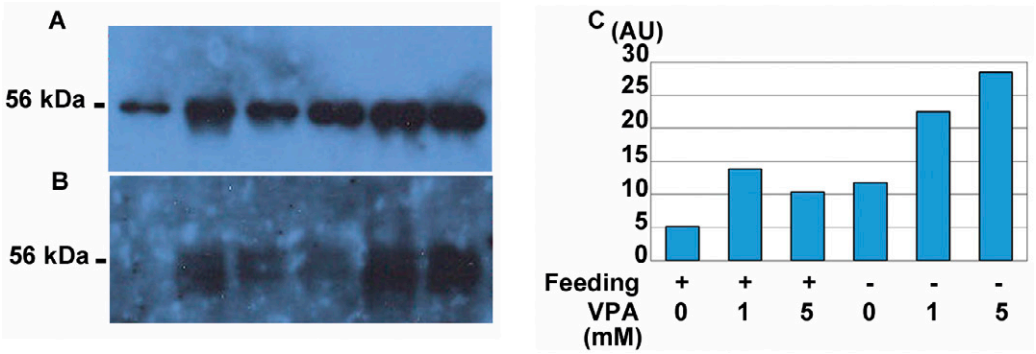

Fig. 1. Detection of acetylated lysines of MDT-28 in fed or starved synchronized L1 larvae and incubated for 4 h with 1 mM VPA or 5 mM VPA or without VPA. Panels **A** and **B** show Western blots of immunoprecipitated GFP::MDT-28 pulled-down by the GFP-Trap system and probed with anti-GFP antibody (panel A) and anti-acetylated lysine antibody (panel B). Panel **C** shows the densitometric analysis of the levels of immunodetected lysine-acetylated GFP::MDT-28 shown in panel B normalized for the expression of GFP::MDT-28 with subtracted background staining and adjusted for loading volumes (10 µl in the first three lanes in panel A representing fed cultures and 20 µl in all the remaining lanes). The Western blot and its analysis is one of two independent experiments with similar results. The densitometric analysis indicates elevated lysine acetylation in larvae cultured in the presence of VPA. The background staining observed in Western blots with anti-acetyl lysine antibody reflects the necessity for long time exposures for the visualization of acetylated lysine, likely indicating that the acetylated GFP::MDT-28 constitutes a minor proportion of the total GFP::MDT-28. The animals were synchronized by starvation after hatching and incubated for 4 hours with or without addition of bacterial food.

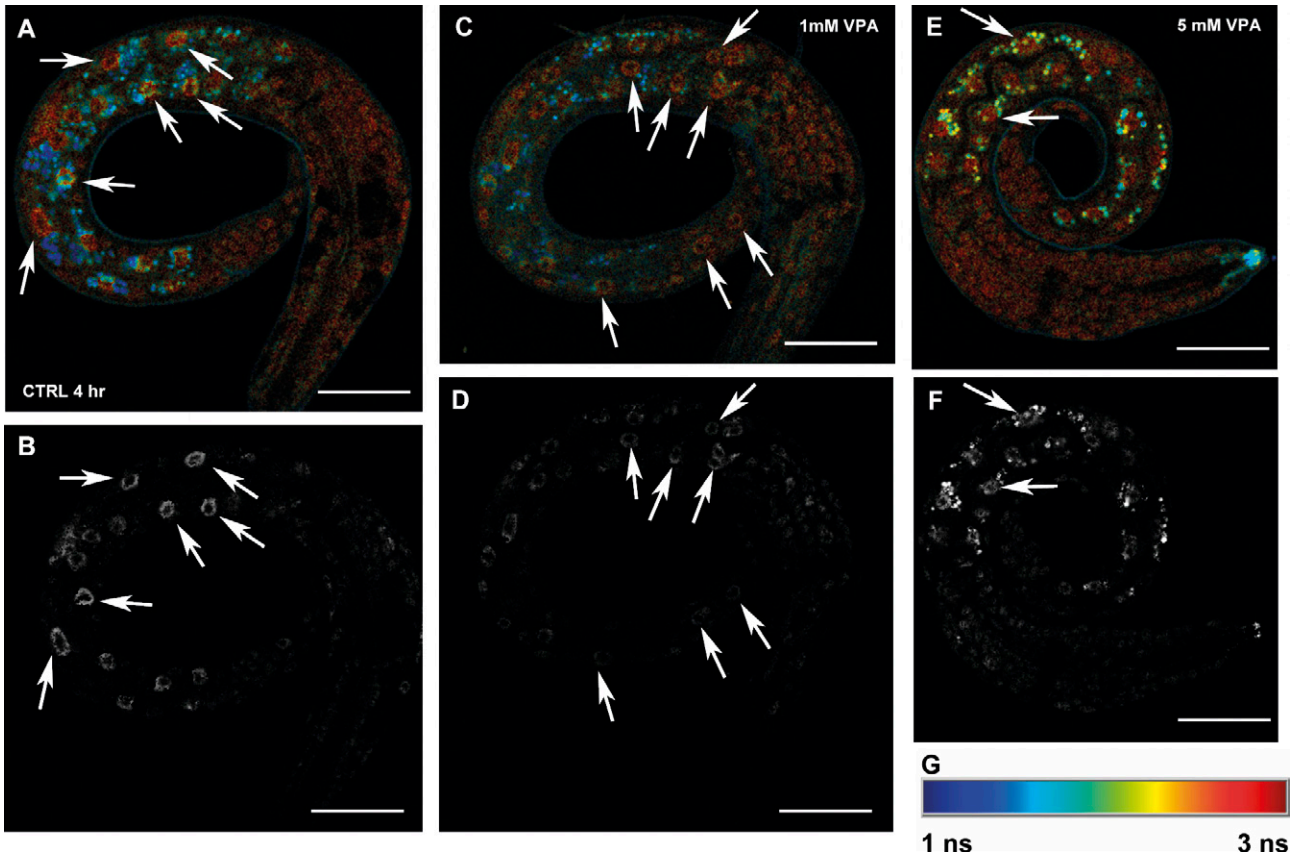

Fig. 2. The effect of short-term (4 h) exposure to VPA on the intracellular distribution of GFP::MDT-28 in synchronized *C. elegans* L1 larvae**.** Panels **A** and **B** show a control L1 larva (no VPA), panels **C** and **D** an L1 larva after treatment with 1 mM VPA, and panels **E** and **F** a larva treated with 5 mM VPA. Panels **A**, **C** and **E** show computed false colour FLIM images. The reference table of average photon arrival time in FLIM images is shown in panel **G**. Panels **B**, **D** and **F** are the red channel images corresponding to the signal from GFP only and show a visible decrease of GFP signal in the larvae incubated with 1 and 5 mM VPA. Bars represent 25 µm.

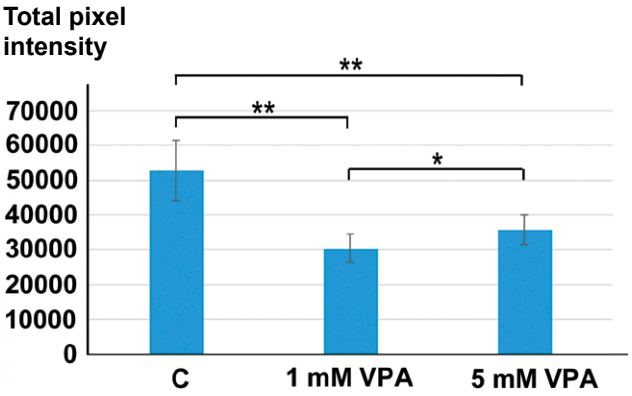

Fig. 3. Densitometric analysis of GFP::MDT-28 FLIM signal in the nuclei of enterocytes of a control larva and larvae incubated with 1 mM and 5 mM VPA for 4 h. The GFP only signal, exported as red channel data obtained for individual nuclei, was analysed densitometrically using the ImageJ program. All clearly defined enterocyte nuclei (N = 35, N = 29 and N = 22, for control nuclei, nuclei of a larva incubated with 1 mM VPA and nuclei of a larva incubated with 5 mM VPA, respectively) were analysed. The values represent total pixel intensity. The P values of the *t*-test of paired sets, for which the null hypothesis is considered as no statistical difference between the two evaluated sets, are as follows: $P = 1.61 \times 10^{-8}$ for control versus 1 mM VPA, $P = 3.67096 \times 10^{-6}$ for control versus 5 mM VPA , P = 0.031745 for 1 mM VPA versus 5 mM VPA. The results show a statistically significant decrease of GFP::MDT-28 in the nuclei of enterocytes treated with 1 and 5 mM VPA versus control nuclei (* < 0.05, ** < 0.00001).

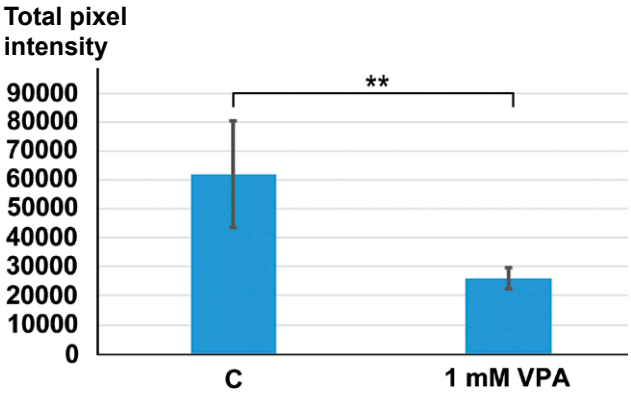

Fig. 5. Densitometric analysis of GFP::MDT-28 FLIM signal in clearly defined enterocyte nuclei of a control larva and a larva incubated with 1 mM VPA for 24 h. The values represent total pixel intensity. The P value of the *t*-test, for which the null hypothesis is considered as no statistical difference between the two evaluated sets, is $P = 4.566 \times 10^{-5}$. The result shows a significant decrease of the GFP::MDT-28 signal in the nuclei of enterocytes after 1 mM VPA treatment (** < 0.0001). N = 26 for control nuclei and N = 20 for nuclei of a larva treated with 1 mM VPA for 24 h.

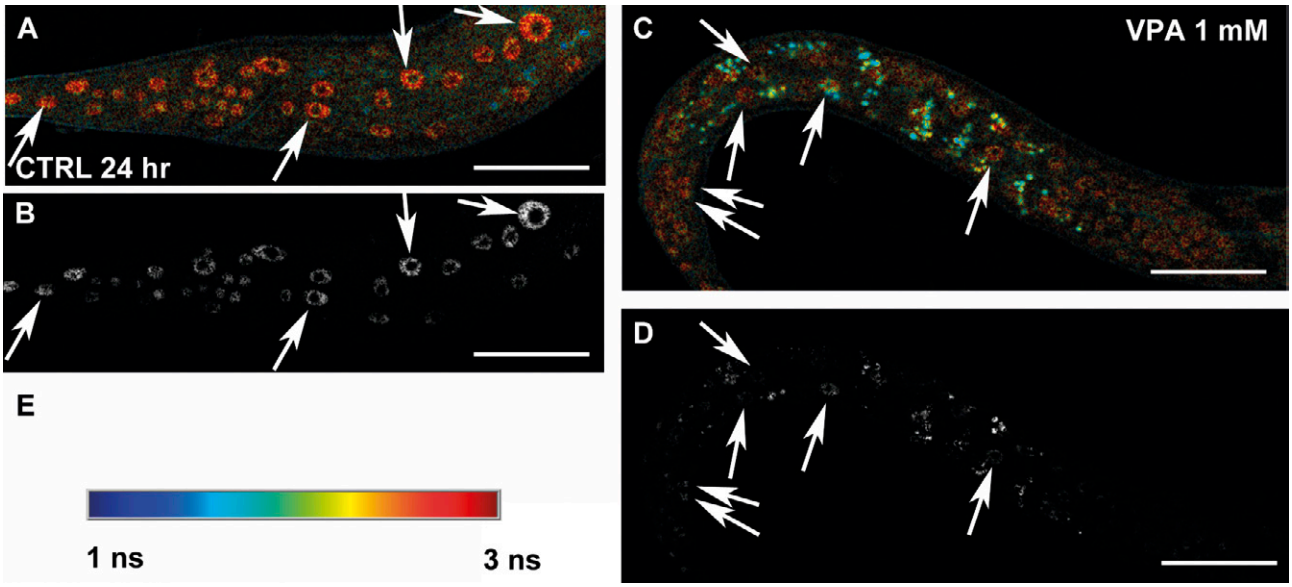

Fig. 4. The effect of 24-h exposure of synchronized *C. elegans* starting from the L1 stage to valproic acid on the intracellular distribution of GFP::MDT-28. Panels **A** and **B** show a control larva and panels **C** and **D** a larva incubated with 1 mM VPA. Panels **A** and **C** show computed false colour FLIM images of the overall signal. The reference table of average photon arrival time in FLIM images is shown in panel **E**. Panels **B** and **D**, derived from the red channel of false colour FLIM images, display intracellular distribution of GFP::MDT-28 and show a visible decrease of the GFP signal in the larva incubated with 1 mM VPA. Bars represent 25 µm.

MED28 has a proven nuclear as well as cytoplasmic localization and functions as a cytoskeleton-associated protein interacting with Grb2 (Wiederhold et al., 2004) and a Mediator subunit in the nucleus (Sato et al., 2004; Beyer et al., 2007). This suggests the possibility that MED28 may bring cytoplasmic regulatory signals towards the regulation of gene expression when its interacting proteins co-localize with MED28 in the nucleus as well. In such a case, translocations of MED28 and its interacting proteins may be part of the regulatory circuits and may have the potential of mediating cell structural signals towards the regulation of gene expression.

In this work we attempted to further characterize MDT-28 that we previously identified in the *C. elegans* genome (Kostrouchova et al., 2017). Analysis of the MDT-28 sequence using bionformatic tools identified MDT-28 along with several other MED28 orthologues as likely targets of lysine acetylation. To test this possibility, we used the GFP-Trap system for immunoprecipitation of GFP::MDT-28 expressed in a transgenic line containing the edited *mdt-28* gene, probed it with a commercially available antibody raised against peptides containing acetylated lysines and confirmed the presence of acetylated lysines in GFP::MDT-28. Treatment with VPA, a known inhibitor of histone deacetylases, increased the proportion of acetylated GFP::MDT-28, indicating that the acetylation of GFP::MDT-28 may be dynamic and is subjected to deacetylation by HDACs sensitive to VPA. We then wanted to know whether exposure of nematodes to VPA affects GFP::MDT-28 *in vivo*. In line with this possibility we detected changes of GFP::MDT-28 intranuclear localization visualized as decreased presence of GFP::MDT-28 in the nuclei and a change of the signal pattern. While under control conditions GFP::MDT-28 was detected in a punctuate intranuclear pattern, treatment with VPA decreased the presence in the punctate centres as well as the overall sum of the GFP signal in the nuclei.

Studies focused on the localization and function(s) of MED28 identified separately its cytoplasmic and nuclear localizations, but rarely reported both localizations. Wiederhold et al. (2004) recognized MED28 (Magicin) cytoplasmic function and interaction with cytoplasmic Grb2 and NF2 tumour-associated protein Merlin and observed MED28 in the cytoplasm associated with actin-containing cytoskeleton. In contrast, studies that identified the nuclear function of MED28 as a component of the Mediator complex proved its localization in the nuclear fractions (Paoletti et al., 2006; Beyer et al., 2007). Our previous work exploited transgenic lines of *C. elegans* carrying MDT-28 fused with GFP under the regulation of the endogenous internal promoter (expressed as MDT-28::GFP from extrachromosomal arrays) and *C. elegans* lines with edited *mdt-28* gene (expressing GFP::MDT-28 from its genomic locus). Both experimental settings proved the dual nuclear and cytoplasmic localization of MDT-28 (Kostrouchova et al., 2017).

Additional data concerning the nuclear and cytoplasmic localization of MED-28 can be found in The Human Protein Atlas. Interestingly, the two antibodies (HPA035900 and HPA035901, produced by Sigma-Aldrich) that were used identified MED28 only rarely (presumably) in the same localization and in the same cell types. The protein species recognized by the two antibodies have sizes of approximately 21, 29, 42, 47 and 63 kDa in the case of HPA035900 and 32, 36 kDa in the case of HPA 035901 (the data was accessed in The Human Protein Atlas on Jan 7, 2018) (Uhlen et al., 2005, 2015, 2017; Thul et al. 2017). Another antibody, MABC1143, anti-MED28 antibody, clone 7E1 available from Merck (Merck & Co, Kenilworth, NJ) recognizes a protein with an approximate size of 20 kDa and gives clear positive signal in both the nuclei and cytoplasm in the mouse blastocyst (Li et al., 2015). These results may reflect extensive posttranslational modification of MDT-28 and selective affinities of antibodies binding to different epitopes on the MDT-28 molecule.

In our experiments, edited MDT-28 (GFP::MDT-28) was expressed as protein species with two close sizes in the expected size range (approximately 56 kDa: GFP 29.6 kDa and MDT-28 22.5 kDa, plus the linker) detected using anti-GFP antibody. The two sizes are likely to reflect posttranslational modifications of MDT-28. Immunodetection of acetylated lysines in GFP::MDT-28 immunoprecipitated by anti-GFP single-chain antibody (using the GFP Trap system) is relatively weak compared to detection obtained by anti-GFP antibody (that differed from the single-chain antibody used in the GFP Trap system). It is possible that the affinity of the antibody raised against acetylated lysines in human H3 histone is relatively low for interaction with acetylated lysines in *C. elegans* MDT-28, but it cannot be ruled out that the proportion of MDT-28 with acetylated lysines may be small and the acetylation of lysines in MDT-28 may be transient and quickly removed. Bioinformatic and experimental studies of Mediator subunits (Nagulapalli et al., 2016) indicated that intrinsically disordered regions and the likelihood for posttranslational modifications are partially conserved, but show tendency to become more complex during evolution in both protein-protein interactions and their modulation by posttranslational modifications. Bioinformatic analysis of lysine acetylation in MDT-28 presented in this study and the presence of intrinsically disordered regions that can be detected by GlobPlot (http://globplot.embl.de/cgiDict.py, accessed on January 7, 2018) (Linding et al., 2003) is well in keeping with the data shown for human MED28 (Nagulapalli et al., 2016) (Fig. 6).

It is still debated whether Mediator complex subunits are in all cells in equimolar stoichiometric ratios, or may be present in different ratios in different cell types or physiological states. The observation of the decrease in the nuclear pool of MDT-28 in response to the treatment with VPA strongly supports variable representation of MDT-28 in the nuclei with ongoing tissue-specific gene expression.

Our results clearly show that MDT-28 nuclear localization is regulated by a mechanism sensitive to VPA.

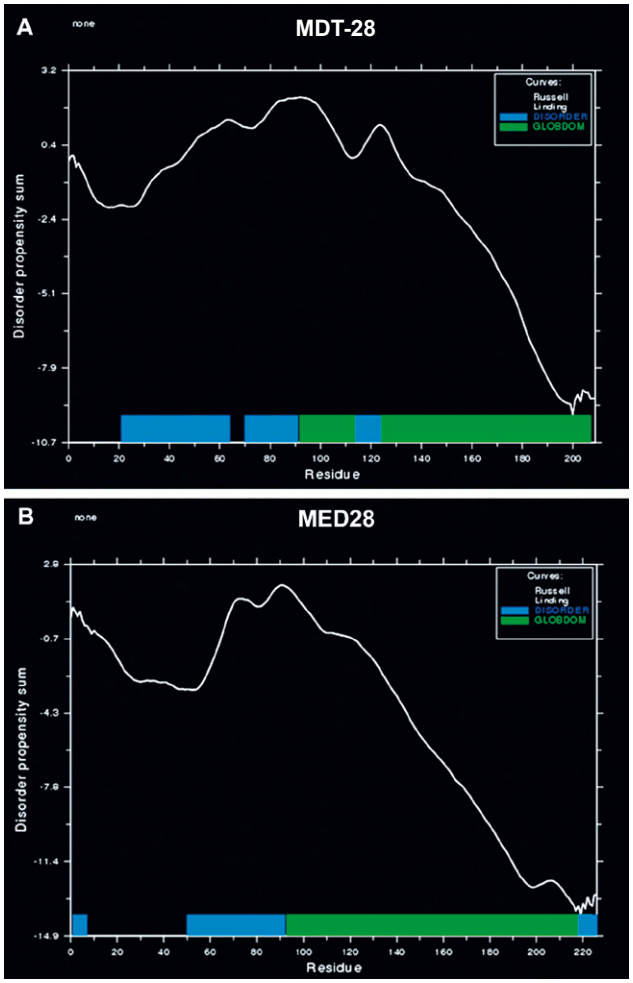

Fig. 6. Schematic representation of intrinsically disordered regions in MDT-28 (panel **A**) and human MED28 (panel **B**). This schematic representation was done using GlobPlot (http://globplot.embl.de/cgiDict.py). Both proteins show similar distribution of intrinsically disordered regions indicated by blue rectangles and structurally organized regions (detected as Globodomains) indicated by green rectangles. The globular domains are recognized as α structured domains in four models obtained by the SWISS-MODEL (https://swissmodel.expasy.org/interactive/ahvMcA/models/, accessed on February 13, 2018) based on templates MED21, RalA-binding protein 1, Apolipoprotein E, and Apolipoprotein A-1. However, high fidelity of the models cannot be expected since no closer templates are available.

VPA was shown to both increase and decrease expression of distinct sets of genes in leukaemia (Stamatopoulos et al., 2009) as well as in non-tumorous cells (Jergil et al., 2011) and was shown to be connected to elevated levels of acetylated histones (reviewed in (Kostrouchova et al., 2007)) and repeatedly reported in many studies (Fukuchi et al., 2009). Increased acetylation in the promoters of histones may well explain the elevated expression of repressed genes, but is unlikely to explain the down-regulation of sets of genes after the treatment with VPA. Our data may indirectly support the existence of Mediator complexes with and without MED28 and the effect of VPA on the composition and function of the Mediator complex. Our results support the possibility that VPA interferes with a mechanism that is involved in the regulation of the intracellular localization of MDT-28.

Acknowledgement

The authors would like to especially thank Zdenek Kostrouch for advice. Please distinguish similar names of coauthors: *Markéta Kostrouchová, ‡ Marta Kostrouchová.

References

Allen, B. L., Taatjes, D. J. (2015) The Mediator complex: a central integrator of transcription. *Nat. Rev. Mol. Cell Biol.* **16**, 155-166.

Benson, D. A., Cavanaugh, M., Clark, K., Karsch-Mizrachi, I., Lipman, D. J., Ostell, J., Sayers, E. W. (2013) GenBank. *Nucleic Acids Res.* **41**, D36-42.

Benson. D. A., Cavanaugh, M., Clark, K., Karsch-Mizrachi, I., Lipman, D. J., Ostell, J., Sayers, E. W. (2017) GenBank. *Nucleic Acids Res.* **45**, D37-D42.

Beyer, K. S., Beauchamp, R. L., Lee, M. F., Gusella, J. F., Naar, A. M., Ramesh, V. (2007) Mediator subunit MED28 (Magicin) is a repressor of smooth muscle cell differentiation. *J. Biol. Chem.* **282**, 32152-32157.

Fukuchi, M., Nii, T., Ishimaru, N., Minamino, A., Hara, D., Takasaki, I., Tabuchi, A., Tsuda, M. (2009) Valproic acid induces up- or down-regulation of gene expression responsible for the neuronal excitation and inhibition in rat cortical neurons through its epigenetic actions. *Neurosci. Res.* **65**, 35-43.

Fuller, P. J., Yang, J., Young, M. J. (2017) 30 YEARS OF THE MINERALOCORTICOID RECEPTOR: Coregulators as mediators of mineralocorticoid receptor signalling diversity. *J. Endocrinol.* **234**, T23-T34.

Grants, J. M., Goh, G. Y., Taubert, S. (2015) The Mediator complex of Caenorhabditis elegans: insights into the developmental and physiological roles of a conserved transcriptional coregulator. *Nucleic Acids Res.* **43**, 2442-2453.

Harper, T. M., Taatjes, D. J. (2017) The complex structure and function of Mediator. *J. Biol. Chem*. doi: 10.1074/jbc.R117.794438

Jergil, M., Forsberg, M., Salter, H., Stockling, K., Gustafson, A. L., Dencker, L., Stigson, M. (2011) Short-time gene expression response to valproic acid and valproic acid analogs in mouse embryonic stem cells. *Toxicol. Sci.* **121**, 328-342.

Kostrouchova, M., Kostrouch, Z., Kostrouchova, M. (2007) Valproic acid, a molecular lead to multiple regulatory pathways. *Folia Biol. (Praha)* **53**, 37-49.

Kostrouchova, M., Kostrouch, D., Chughtai, A. A., Kassak, F., Novotny, J. P., Kostrouchova, V., Benda, A., Krause, M. W., Saudek, V., Kostrouchova, M., Kostrouch, Z. (2017) The nematode homologue of Mediator complex subunit 28, F28F8.5, is a critical regulator of C. elegans development. *PeerJ.* **5**, e3390.

Kulak, N. A., Pichler, G., Paron, I., Nagaraj, N., Mann, M. (2014) Minimal, encapsulated proteomic-sample process-

ing applied to copy-number estimation in eukaryotic cells. *Nat. Methods* **11**, 319-324.

Lee, M. F., Beauchamp, R. L., Beyer, K. S., Gusella, J. F., Ramesh, V. (2006) Magicin associates with the Src-family kinases and is phosphorylated upon CD3 stimulation. *Biochem. Biophys. Res. Commun.* **348**, 826-831.

Li, A., Xue, Y., Jin, C. J., Wang, M. H., Yao, X. B. (2006) Prediction of N- ε-acetylation on internal lysines implemented in Bayesian Discriminant Method. *Biochem. Biophys. Res. Commun.* **350**, 818-824.

Li, L., Walsh, R. M., Wagh, V., James, M. F., Beauchamp, R. L., Chang, Y. S., Gusella, J. F., Hochedlinger, K. Ramesh, V. (2015) Mediator subunit Med28 is essential for mouse peri-implantation development and pluripotency. *PLoS One* **10**, e0140192.

Linding, R., Russell, R. B., Neduva, V., Gibson, T. J. (2003) GlobPlot: exploring protein sequences for globularity and disorder. *Nucleic Acids Res.* **31**, 3701-3708.

Liu, C., Zhang, L., Shao, Z. M., Beatty, P., Sartippour, M., Lane, T. F., Barsky, S. H., Livingston, E., Nguyen, M. (2002) Identification of a novel endothelial-derived gene EG-1. *Biochem. Biophys. Res. Commun.* **290**, 602-612.

McClatchey, A. I., Giovannini, M. (2005) Membrane organization and tumorigenesis – the NF2 tumor suppressor, Merlin. *Genes Dev.* **19**, 2265-2277.

McClatchey, A. I., Fehon, R. G. (2009) Merlin and the ERM proteins – regulators of receptor distribution and signaling at the cell cortex. *Trends Cell. Biol.* **19**, 198-206.

Nagulapalli, M., Mají, S., Dwivedi, N., Dahiya, P., Thakur, J. K. (2016) Evolution of disorder in Mediator complex and its functional relevance. *Nucleic Acids Res.* **44**, 1591-1612.

Paoletti, A. C., Parmely, T. J., Tomomori-Sato, C., Sato, S., Zhu, D., Conaway, R. C., Conaway, J. W., Florens, L., Washburn, M. P. (2006) Quantitative proteomic analysis of distinct mammalian Mediator complexes using normalized spectral abundance factors. *Proc. Natl. Acad. Sci. USA* **103**, 18928-18933.

Poss, Z. C., Ebmeier, C. C., Taatjes, D. J. (2013) The Mediator complex and transcription regulation. *Crit. Rev. Biochem. Mol. Biol.* **48**, 575-608.

Reinke, V., Krause, M., Okkema, P. (2013) Transcriptional regulation of gene expression in C. elegans. *WormBook* 1-34.

Sato, S., Tomomori-Sato, C., Parmely, T. J., Florens, L., Zybailov, B., Swanson, S. K., Banks, C. A., Jin, J., Cai, Y., Washburn, M. P., Conaway, J. W., Conaway, R. C. (2004) A set of consensus mammalian mediator subunits identified by multidimensional protein identification technology. *Mol. Cell* **14**, 685-691.

Stamatopoulos, B., Meuleman, N., De Bruyn, C., Mineur, P., Martiat, P., Bron, D., Lagneaux, L. (2009) Antileukemic activity of valproic acid in chronic lymphocytic leukemia B cells defined by microarray analysis. *Leukemia* **23**, 2281-2289.

Syring, I., Klumper, N., Offermann, A., Braun, M., Deng, M., Boehm, D., Queisser, A., von Massenhausen, A., Bragelmann, J., Vogel, W., Schmidt, D., Majores, M., Schindler, A., Kristiansen, G., Muller, S. C., Ellinger, J., Shaikhibrahim, Z., Perner, S. (2016) Comprehensive analysis of the transcriptional profile of the Mediator complex across human cancer types. *Oncotarget* **7**, 23043-23055.

Thul, P. J., Akesson, L., Wiking, M., Mahdessian, D., Geladaki, A., Ait Blal, H., Alm, T., Asplund, A., Bjork, L., Breckels, L. M., Backstrom, A., Danielsson, F., Fagerberg, L., Fall, J., Gatto, L., Gnann, C., Hober, S., Hjelmare, M., Johansson, F., Lee, S., Lindskog, C., Mulder, J., Mulvey, C. M., Nilsson, P., Oksvold, P., Rockberg, J., Schutten, R., Schwenk, J. M., Sivertsson, A., Sjostedt, E., Skogs, M., Stadler, C., Sullivan, D. P., Tegel, H., Winsnes, C., Zhang, C., Zwahlen, M., Mardinoglu, A., Ponten, F., von Feilitzen, K., Lilley, K. S., Uhlen, M., Lundberg, E. (2017) A subcellular map of the human proteome. *Science* **356**, 10.1126/science.aal3321.

Tsai, K. L., Sato, S., Tomomori-Sato, C., Conaway, R. C., Conaway, J. W., Asturias, F. J. (2013) A conserved Mediator-CDK8 kinase module association regulates Mediator-RNA polymerase II interaction. *Nat. Struct. Mol. Biol.* **20**, 611-619.

Uhlen, M., Bjorling, E., Agaton, C., Szigyarto, C. A., Amini, B., Andersen, E., Andersson, A. C., Angelidou, P., Asplund, A., Asplund, C., Berglund, L., Bergstrom, K., Brumer, H., Cerjan, D., Ekstrom, M., Elobeid, A., Eriksson, C., Fagerberg, L., Falk, R., Fall, J., Forsberg, M., Bjorklund, M. G., Gumbel, K., Halimi, A., Hallin, I., Hamsten, C., Hansson, M., Hedhammar, M., Hercules, G., Kampf, C., Larsson, K., Lindskog, M., Lodewyckx, W., Lund, J., Lundeberg, J., Magnusson, K., Malm, E., Nilsson, P., Odling, J., Oksvold, P., Olsson, I., Oster, E., Ottosson, J., Paavilainen, L., Persson, A., Rimini, R., Rockberg, J., Runeson, M., Sivertsson, A., Skollermo, A., Steen, J., Stenvall, M., Sterky, F., Stromberg, S., Sundberg, M., Tegel, H., Tourle, S., Wahlund, E., Walden, A., Wan, J., Wernerus, H., Westberg, J., Wester, K., Wrethagen, U., Xu, L. L., Hober, S., Ponten, F. (2005) A human protein atlas for normal and cancer tissues based on antibody proteomics. *Mol. Cell. Proteomics* **4**, 1920-1932.

Uhlen, M., Fagerberg, L., Hallstrom, B. M., Lindskog, C., Oksvold, P., Mardinoglu, A., Sivertsson, A., Kampf, C., Sjostedt, E., Asplund, A., Olsson, I., Edlund, K., Lundberg, E., Navani, S., Szigyarto, C. A., Odeberg, J., Djureinovic, D., Takanen, J. O., Hober, S., Alm, T., Edqvist, P. H., Berling, H., Tegel, H., Mulder, J., Rockberg, J., Nilsson, P., Schwenk, J. M., Hamsten, M., von Feilitzen, K., Forsberg, M., Persson, L., Johansson, F., Zwahlen, M., von Heijne, G., Nielsen, J., Ponten, F. (2015) Proteomics. Tissue-based map of the human proteome. *Science* **347**, 1260419.

Uhlen, M., Zhang, C., Lee, S., Sjostedt, E., Fagerberg, L., Bidkhori, G., Benfeitas, R., Arif, M., Liu, Z., Edfors, F., Sanli, K., von Feilitzen, K., Oksvold, P., Lundberg, E., Hober, S., Nilsson, P., Mattsson, J., Schwenk, J. M., Brunnstrom, H., Glimelius, B., Sjoblom, T., Edqvist, P. H., Djureinovic, D., Micke, P., Lindskog, C., Mardinoglu, A.,Ponten, F. (2017) A pathology atlas of the human cancer transcriptome. *Science* **357**. 10.1126/science.aan2507

Wiederhold, T., Lee, M. F., James, M., Neujahr, R., Smith, N., Murthy, A., Hartwig, J., Gusella, J. F., Ramesh, V. (2004) Magicin, a novel cytoskeletal protein associates with the NF2 tumor suppressor merlin and Grb2. *Oncogene* **23**, 8815-8825.

Yin, J. W., Wang, G. (2014) The Mediator complex: a master coordinator of transcription and cell lineage development. *Development* **141**, 977-987.

JOURNAL OF PROTEOMICS 110 (2014) 93–106

Available online at www.sciencedirect.com

ScienceDirect

www.elsevier.com/locate/jprot

SKIP and BIR-1/Survivin have potential to integrate proteome status with gene expression

David Kostrouch[a], *Markéta Kostrouchová*[a], *Petr Yilma*[a], *Ahmed Ali Chughtai*[a], *Jan Philipp Novotný*[a], *Petr Novák*[b], *Veronika Kostrouchová*[a], *Marta Kostrouchová*[c], *Zdeněk Kostrouch*[a,*]

[a]*Laboratory of Molecular Pathology, Institute of Cellular Biology and Pathology, First Faculty of Medicine, Charles University in Prague, Czech Republic*
[b]*Laboratory of Structure Biology and Cell Signaling, Institute of Microbiology, Czech Academy of Sciences, Vídeňská 1083, Prague, Czech Republic*
[c]*Laboratory of Molecular Biology and Genetics, Institute of Cellular Biology and Pathology, First Faculty of Medicine, Charles University in Prague, Czech Republic*

ARTICLE INFO

Article history:
Received 12 May 2014
Accepted 22 July 2014
Available online 1 August 2014

Keywords:
BIR-1
Gene expression
Ribosomal stress
SKIP
Survivin
Proteome

ABSTRACT

SKIP and BIR are evolutionarily conserved proteins; SKIP (SKP-1) is a known transcription and splicing cofactor while BIR-1/Survivin regulates cell division, gene expression and development. Their loss of function induces overlapping developmental phenotypes. We searched for SKP-1 and BIR-1 interaction on protein level using yeast two-hybrid screens and identified partially overlapping categories of proteins as SKIP-1 and BIR-1 interactors. The interacting proteins included ribosomal proteins, transcription factors, translation factors and cytoskeletal and motor proteins suggesting involvement in multiple protein complexes. To visualize the effect of BIR-1 on the proteome in *Caenorhabditis elegans* we induced a short time pulse BIR-1 overexpression in synchronized L1 larvae. This led to a dramatic alteration of the whole proteome pattern indicating that BIR-1 alone has the capacity to alter the chromatographic profile of many target proteins including proteins found to be interactors in yeast two hybrid screens. The results were validated for ribosomal proteins RPS3 and RPL5, non-muscle myosin and TAC-1, a transcription cofactor and a centrosome associated protein. Together, these results suggest that SKP-1 and BIR-1 are multifunctional proteins that form multiple protein complexes in both shared and distinct pathways and have the potential to connect proteome signals with the regulation of gene expression.

Biological significance

The genomic organization of the genes encoding BIR-1 and SKIP (SKP-1) in *C. elegans* have suggested that these two factors, each evolutionarily conserved, have related functions. However, these functional connections have remained elusive and underappreciated in light of limited information from *C. elegans* and other biological systems. Our results provide further evidence for a functional link between these two factors and suggest they may transmit proteome signals towards the regulation of gene expression.

© 2014 Elsevier B.V. All rights reserved.

* *Corresponding author at:* Laboratory of Molecular Pathology, Institute of Cellular Biology and Pathology, First Faculty of Medicine, Charles University in Prague, Ke Karlovu 2, 128 00 Prague 2, Czech Republic. Tel.: +420 22496 7090; fax: +420 22496 7092.
E-mail address: zdenek.kostrouch@lf1.cuni.cz (Z. Kostrouch).

http://dx.doi.org/10.1016/j.jprot.2014.07.023
1874-3919/© 2014 Elsevier B.V. All rights reserved.

1. Introduction

Regulation of gene expression is the basis of proper function of organisms, their development and metabolism. It is executed at the level of chromatin by transcription factors, which recognize and bind specific regions in promoters of genes, and in cooperation with transcription cofactors attract and activate Polymerase II complex proteins. Further, downstream mechanisms then modulate gene expression at the level of RNA splicing and mRNA processing, nuclear export and translation into proteins. Tissue and metabolic state specific transcription factors and cofactors that are expressed in response to specific developmental and metabolic stimuli direct proper gene expression to cope with particular developmental and metabolic needs at the level of cells, tissues and whole organisms. This basic regulatory network is likely to include additional mechanisms that sense the functional and structural cellular states and link them with gene expression regulation for achievement of a precise and fast regulatory response.

SKIP is an ancient transcription cofactor found in all multicellular organisms as well as in yeast. It was originally identified as BX42, a *Drosophila* nuclear protein associated with active transcription (puffs) on polytene chromosomes [1,2] and later found in many species including *Dictyostelium discoideum* [3] and yeast [4]. SKIP interacts with several transcription factors including nuclear receptors [5–8], Notch [9], Wnt/beta catenin [10], TGF beta and Smad protein complexes [11] and it was also identified as a component of splicing machinery in yeast, mammals [12] and plants [13]. It was identified in both transcription activating as well as transcription inhibiting complexes [14]. In *Caenorhabditis elegans*, SKIP is indispensable for normal development and its inhibition results in multiple phenotypes including larval transition and molting that is dependent on NHR-23 [15].

In *C. elegans*, SKIP (SKP-1) is organized in an operon together with a mitotic and microtubule organizing protein BIR-1 [15], a homologue of the vertebrate protein Survivin that is expressed predominantly in fast dividing cells and is found upregulated in most if not all human cancers [16]. Since operons ensure that co-organized genes are co-expressed, at least at the transcriptional level, we hypothesized that these two proteins may be linked functionally. We previously showed in *C. elegans* that both BIR-1 and SKIP are involved in the regulation of gene expression and development. Moreover, in a heterologous transfection system with thyroid receptor/tri-iodothyronine, these factors act cooperatively in activating expression [17].

In this study, we sought to identify SKP-1 and BIR-1 involvement in a protein regulatory network by searching for their interacting proteins using yeast two-hybrid screens. Surprisingly, this strategy indicated that SKP-1 and BIR-1 interact with a wide variety of partially overlapping categories of proteins but not directly with each other. The regulatory potential of BIR-1 was visualized using a short time overproduction of BIR-1 in synchronized *C. elegans* larvae and by a whole proteome differential display. This confirmed that elevated levels of BIR-1 project to immediate whole proteome changes. The results were validated for ribosomal proteins RPS3 and RPL5, non-muscle myosin and TAC-1, a transcription cofactor and a centrosome associated protein implicated in cancer. Our results show that SKP-1 and BIR-1 are linked more than previously thought. They have potential to link the proteome status with major cellular regulatory pathways including gene expression, ribosomal stress pathway, apoptosis and cell division. SKP-1 and BIR-1 may be regarded as proteome sensors.

2. Materials and methods

2.1. Experimental design

Screening for interacting proteins of BIR-1 and SKP-1 was performed using the ProQuest Two-Hybrid System with Gateway Technology purchased from Invitrogen (Carlsbad, California, USA). Potential direct interactions between BIR-1 and SKP-1 were analyzed using the same system. The effect of a short-time forced expression of BIR-1 on the near-complete proteome of nondividing cells of *C. elegans* L1 larvae was visualized by two dimensional comparative chromatography using the Proteome fractionation system from Beckman Coulter (Brea, CA, USA) and fractions with differential protein content were visualized by DeltaVue software and were further examined by mass spectrometry. Selected proteins identified as BIR-1 and SKP-1 interacting proteins or proteomic targets of BIR-1 were analyzed in pull-down experiments using BIR-1 and SKP-1 GST-fusion proteins. Analyzed target proteins were expressed in vitro using the reticulocyte TNT system from Promega (Fitchburg, WI, USA) and labeled by ^{35}S-methionine (Institute of Isotopes Co., Budapest, Hungary). Bound interacting proteins were detected by Liquid scintillation analyzer Tri-Carb 1600TR Packard (Meriden, CT, USA). The effect of BIR-1 short-time overexpression on selected candidate interacting proteins was visualized using immunohistochemistry or by functional studies of cell cycle and apoptosis (employing immunohistochemistry and lines carrying integrated GFP fusion transgenes).

2.1.1. Strains used in the study

The *C. elegans* Bristol N2 strain was used whenever not specifically stated and was maintained as described [18]. For visualization of chromatin structure, the line AZ212 expressing Histone H2B::GFP was used.

BIR-1 overexpressing worms were created as lines expressing *bir-1* mRNA from heat-shock regulated promoter and were prepared by amplifying *bir-1* cDNA from wild-type mRNA. Sub-cloned and sequence verified constructs were cloned into the heat-shock promoter vector pPD49.83. 100 ng/μl of plasmid DNA was microinjected along with a marker plasmid pPRF4, *rol-6* (*su10060*) using an Olympus IX70 inverted microscope (Olympus, Tokyo, Japan) equipped with a PC-10 Narishige Microinjection System (Narishige, Tokyo, Japan).

2.2. Yeast two-hybrid screens

To identify BIR-1 and SKP-1 interacting proteins, we used the ProQuest Two-Hybrid System with Gateway Technology purchased from Invitrogen. The *C. elegans* mixed stages (Bristol N2) library (originally made by Monique A. Kreutzer and Sander van den Heuvel) was purchased from Invitrogen (Cat. No. 11288-016). *bir-1* and *skp-1* cDNAs were amplified

from N2 mixed stages cDNA using primers having flanking sequences ATT and ligated into the pENTRY vector. After cloning the cDNAs, the inserts containing complete coding regions were transferred into pDEST™32 vector using Clonase leading to DBX constructs (bait vectors) creating BIR-1 and SKP-1 fused to GAL4 DNA binding domain. These vectors were used for screening of the *C. elegans* cDNA library after testing for self activation of both *bir-1* and *skp-1* bait vectors.

The vector pDEST 32 includes the GAL DNA binding domain, the ARS/CEN6 sequence for replication and maintenance of low copy numbers in yeast, the LEU2 gene for selection in yeast on medium lacking leucine, the constitutive moderate-strength promoter and transcription terminator of the yeast Alcohol Dehydrogenase gene (ADH1) to drive expression of the GAL4 DBD bait fusion, the dominant CYH 2S allele that confers sensitivity to cycloheximide in yeast for plasmid shuffling, a pUC-based replication origin and gentamicin resistance gene (Gmr) for replication and maintenance in *Escherichia coli*.

For the analysis of BIR-1 binding to SKP-1, pDEST™22 vector containing a GAL4 Activation Domain (GAL4 AD) containing Gateway® Destination Vector was used.

Similarly, the constructs for SKP-1 were prepared using the same vectors. To reduce false positive interactants, the "Three Reporter Genes" system was used (HIS3, URA3 and lacZ stably integrated in the yeast genome). Additional controls included yeast control strains A to E, a self-activation test of the bait constructs, and a test of growth on histidine deficient media. For both BIR-1 and SKP-1 interacting proteins a total of 250 μl of competent cells containing more than 10^6 transformants were acquired. Screening yielded 54 colonies for SKP-1 and approximately 30 for BIR-1 that were prepared as yeast minipreps, screened by PCR using primers 5036 and 5037 (derived from pPC86 vector) and sequenced. All sequences were controlled for proper frame ligation of the insert by sequencing.

2.3. Two-dimensional comparative chromatography

Two-dimensional chromatographic separation of worm lysates was performed on the ProteomeLab PF 2D Protein Fractionation System (Beckman Coulter, Inc., Fullerton, CA) as recommended by the manufacturer. The chromatograms were analyzed using computer software provided by the manufacturer.

In order to detect differences in proteomes of mutant and wild-type larvae we prepared total protein from synchronized, bleached N2 L1 worms and homozygous *bir-1* animals. Proteomes were then analyzed using PF2D. In the first dimension all proteins were separated into 37 fractions by chromatofocusing, according to their isoelectric point, and eluted by a pH gradient. Proteins with an isoelectric point below pH 4.0 were then eluted by a rising concentration of NaCl (by rising ionic strength). Each of the 37 fractions was then further separated into an additional 35 fractions in the second dimension according to hydrophobicity by reversed-phase chromatography.

2.3.1. Preparation of protein lysates

In order to prepare larvae overexpressing *bir-1* in a short time period, we prepared embryos from transgenic hermaphrodites carrying *bir-1* gene regulated by hear-shock responding promoter. Synchronized L1 larvae were prepared by food deprivation. Control larvae were prepared in the same way. Larvae were then exposed to 37 °C for 20 min, left for 20 min at room temperature to recover and incubated for an additional 30 min at 37 °C. Larvae were than pelleted by centrifugation and frozen in aliquots. In order to obtain sufficient amount of material, these experiments had to be repeated 20 times over the period of 3 month. Control larvae were prepared in parallel in the same number of individual experiments. For preparation of protein lysates, frozen samples were melted on wet ice, pooled in 0.2 ml of 50 mM Tris–HCL (pH 8.0) and vortexed. The samples were then mixed with 1.6 ml of lysis buffer (7.5 M urea, 2.5 M thiourea, 12.5% glycerol, 50 mM Tris, 2.5% n-octylglucoside, 6.25 mM Tris-(carboxyethyl) phosphine hydrochloride containing 1× Protease Inhibitor Cocktail (Boehringer Mannheim, Mannheim, Germany)). The suspensions were incubated on ice for 10 min and sonicated in five cycles, each consisting of four times 10 s sonication/10 s interruption (20 kHz, amplitude 20 μm, 60 W) (Ultrasonic Processor (Cole-Parmers Instruments, Vernon Hills, IL)) using the internal sonication rod. The suspension was cleared from the non-soluble material by centrifugation at 20,000 ×*g* for 60 min at 4 °C and the supernatants were harvested. For subsequent first and second dimension chromatographic separations, the Beckman ProteomeLab PF 2D kit (part No. 380977) (Beckman Coulter, Inc., Fullerton, CA) was used. The sample was supplemented with Start Buffer to a final volume of 2.5 ml. The lysis buffer was then exchanged for the Start Buffer supplied by Beckman using the PD10 column (Amersham Pharmacia Biosciences, Uppsala, Sweden) equilibrated with Start Buffer for the first dimension separation (pH 8.5 ± 0.1, pH adjusted with iminodiacetic acid and ammonium hydroxide). The samples were loaded onto the PD10 columns, the first eluents were discarded. Start Buffer was used to elute the proteins that were collected in the first 3.5 ml fractions. The protein content was estimated using a BCA kit (Pierce, Rockford, IL) (C = 0.62 μg/μl for *bir-1* overexpression and C = 1.06 μg/μl for controls). 1.2 mg of total protein was loaded into the First Dimension Module in a total volume of 2 ml (the volume for control protein lysate was increased to 2 ml using 1× Start Buffer).

2.3.2. First dimension — chromatofocusing HPLC (HPCF)

For the chromatofocusing separation, the first module of the Beckman Coulter ProteomeLab PF 2D system was used (Beckman Coulter, Inc., Fullerton, CA). The HPCF column was equilibrated with 25 column volumes of Start Buffer. The pH gradient was based on the buffers supplied by the manufacturer, the Start Buffer and the Elution Buffer (Beckman Coulter, Inc.; pH adjusted with iminodiacetic acid and ammonium hydroxide). The upper limit of the pH gradient was set by the Start Buffer (pH 8.5) and the lower limit was set by the Elution Buffer (pH 4.0). The pH was monitored using a flow-through on-line probe. Following the pH gradient elution, the proteins remaining in the column were eluted by increasing ionic strength gradient (based on 1 M and 5 M NaCl). Protein content in eluates was determined by UV absorbance at 280 nm. Fractions were collected in 96 well plates (2 ml well capacity). The chromatofocusing fractionation was based on first on time for the first 9 fractions (5 minute intervals), then on pH (in the range of pH 8.5 to 4.0, 17 fractions, steps of pH approximately 0.27) and finally on

ionic strength (1 M NaCl to 5 M NaCl) for the last 14 fractions. The fractions were collected by Beckman Coulter FC/I Module (Fraction collector/injector). The reproducibility of the first (and the second dimension) separation was tested using control material assayed by Western blots for selected nuclear hormone receptors and was satisfactory for both dimensions. A ProteomeLab PF 2D kit containing new buffers and columns was used for the first dimension separation of control proteome and BIR-1 overexpression proteome and both analyses were done in the same day after careful wash and equilibration of the first dimension chromatofocusing HPLC (HPCF) system in an air-conditioned laboratory at 23 °C.

2.3.3. Second dimension — reversed phase HPLC (HPRP — High Performance Reversed Phase Chromatography)

The second module of Beckman Coulter ProteomeLab PF 2D system was used for the separation of proteins according to the surface hydrophobicity with two solvents. Solvent A was 0.1% trifluoroacetic acid (TFA) in water and solvent B was 0.08% TFA in acetonitrile. The aliquots of first dimension fractions were separated on HPRP columns packed with nonporous silica beads at 50 °C. The module was equilibrated with solvent A for 10 min. The gradient was run from 0 to 100% of solvent B for 35 min, followed by an elution with solvent B for 5 min to elute the remaining proteins from the column. The fractions were collected at 1 minute intervals (at the flow rate 0.2 ml/min) into 96 well plates (2 ml well capacity) using Fraction collector FC 204 (Gilson, Inc., Middleton, WI, USA). The module was then washed and equilibrated with solvent A by a 10 minute run and prepared for second dimension separation of another first dimension separation fraction. Fractions were frozen before following mass spectrometry analysis. A total of 1260 fractions were collected for each control proteome and the proteome of BIR-1 overexpressing larvae.

Chromatograms from corresponding paired fractions were then analyzed using 32Karat software. ProteoVue and DeltaVue software enabled us to represent differentially the entire proteome and also individual fractions. Some paired samples required manual compensation for a higher baseline.

The 98 paired fractions that showed prominent differences in major chromatographic peaks were selected for further analysis by mass spectrometry to identify their protein components. Chromatographic fractions that corresponded to identified peaks of paired fractions were prepared and analyzed using liquid chromatography–tandem mass spectrometry (LC/MS/MS) to identify present proteins by peptide microsequencing to derive sequences of individual proteins.

Specific fractions that were chosen for further analysis by mass spectrometry were prepared in the following manner — fractions were dried down into pellets (speed vac), these pellets were then dissolved in 15 μl of cleavage buffer which contained 0.01% 2-mercaptoethanol (Sigma Aldrich, St. Louis, MO, USA), 0.05 M 4-ethylmorpholine acetate pH 8.1 (Fluka (Sigma Aldrich)), 5% MeCN (Merck, Whitehouse Station, NJ, USA), and 10 ng/μl of sequencing grade trypsin (Promega). Digestion was carried out at 37 °C overnight and the resultant peptides were subjected to analysis by mass spectrometry.

Five microliters of the mixture was applied on a Magic-C18 column, (0.180 × 150 mm, 200 Å, 5 μm — Michrom Bioresources, Auburn, CA) and separated by gradient elution. The column was connected to a LCQ^{DECA} ion trap mass spectrometer (ThermoQuest, San Jose, CA) and equipped with a nanoelectrospray ion source. Spectrum analysis was done using SEQUEST™ software against the SwissProt database. SEQUEST results were processed with BioWorks Browser software [19] using the following criteria: XCorr values were 1.7 for singly charged, 2.2 for doubly charged and 3.0 for triply charged peptides [20].

2.4. Bioinformatic analysis

Bioinformatic analysis was done using NCBI bioinformatic tools BLAST [21], gene ontology tool DAVID (http://david.abcc.ncifcrf.gov/) [22,23] and Wormbase WS242 (http://www.wormbase.org). GO terms with the enrichment factor bigger than 2 were considered as significant. Curated GO terms keeping with known functions of either BIR-1 of SKP-1 were considered as criteria of shared functions.

2.5. Pull-down experiments for selected proteins

The complete cDNA of BIR-1 and SKP-1 (not including the first methionine codon) was amplified by PCR and cloned into the pGEX-2T vector (Amersham Pharmacia Biotech, Amsterdam, UK) and sequenced. The GST fusion proteins (Glutathione-S-transferase) were expressed in the BL-21 strain of *E. coli*. Empty pGEX-2T vectors expressing the protein domain of GST were used for control experiments. Cultures of transformed bacteria that were obtained from single bacterial colonies were grown overnight at 37 °C in 400 ml of Luria–Broth medium with 100 μg/ml of Ampicillin. Cultures were grown to an O.D. (600 nm) of 0.8 and subsequently induced by 1 mM isopropyl-thiogalactopyranoside (IPTG), incubated at 20 °C for 5 h and centrifuged to pellets at 3300 ×*g* at 4 °C for 10 min. The pellets were washed twice in LB medium and then resuspended in 6 ml of phosphate-buffered saline (PBS). Cell lysis of bacteria was performed in 6 ml of Lysis buffer (Biorad — 2× Native lysis buffer, CA), that was supplemented with protease inhibitors (1× Complete, Roche, Penzberg, Germany). The samples were incubated on ice for 10 min with intermittent vortexing and sonication (4× for 10 s at 80% intensity) — (Sonicator UP 100 H, Hielscher, Teltow, Germany). The lysates were centrifuged at 10,000 RPM for 5 min. at 4 °C. The supernatant was removed and filtered by ROTH 0.22 μm filter (Carl Roth GmbH, Karlsruhe, Germany). Glutathione–agarose (Sigma-Aldrich, St. Louis, Mo) was used for the binding of GST, GST-SKIP and GST-BIR and was prepared by swelling 0.01 g of beads in 1 ml of PBS, which were then collected by sedimentation and then resuspended in 100 μl of PBS. Purification of fusion proteins and control was done in 100 μl of slurry, 300 μl of bacterial lysates that were incubated for 30 min at 4 °C, and mixed intermittently (every 4 min). Next the beads were washed 4 times in 1 ml of PBS Triton X-100 (1%). Beads were collected by sedimentation and resuspended in 500 μl of PBS. Elution was done in 10 mM reduced glutathione and 50 mM Tris–HCL, pH 9.5 (all chemicals were obtained from Sigma-Aldrich).

The TNT T7/T3 coupled reticulocyte lysate system (Promega) was used to prepare ^{35}S-radiolabeled proteins with 1.48 MBq of ^{35}S-Methionine (37 TBq/mmol) in the final volume of 50 μl (Institute of Isotopes, Budapest, Hungary). Binding was done at 22 °C for 30 min using 10 μl of the TNT

product — mixing every 4 min and then the samples were washed 3× in 1 ml of PBS and resuspended in 40 μl of PBS. Afterwards 5 μl of 2× Laemmli Buffer and 1 μl of β-mercaptoethanol were added. The samples were boiled for 5 min. 35 μl of the sample was used for polyacrylamide gel electrophoresis and autoradiography. 10 μl of supernatant was analyzed using the Liquid Scintillation Analyzer Tri-Carb 1600 TR (Packard, Meriden, CT) and Ultima-Gold scintillation cocktail (Perkin-Elmer, Watham, MA). For determination of input in binding experiments, 2 μl of in-vitro transcribed — translated product was resolved using polyacrylamide gel electrophoresis, transferred on Whitman 3M paper, dried and radioactivity determined in cut strips containing the translated proteins but not the unincorporated ^{35}S-Methionine.

2.6. *skp-1* reduction-of-function effect

The knockdown of *skp-1* was induced by injecting *skp-1* specific dsRNA directly into the gonads of adult wild type N2 hermaphrodites. The progeny was harvested and stained with DAPI and by antibody staining (9 v 5 LA) against SPD-2 that localizes to centrosomes (denominated 9 v 5, LA) (a kind gift of Dr. O'Connell) [24] and used diluted 1:100. We searched for phenotypic changes described earlier [15] and we added screening for cell cycle arrest phenotypes.

2.7. Antibody staining

Antibody experiments (for NMY-2) were done on transgenic embryos and larvae (expressing *bir-1* from heat shock regulated promoter) that were bleached, heated for 30 min at 34 °C and allowed 1 h for recovery at room temperature. Controls were wild type N2 embryos and larvae prepared and heated in parallel to experimental embryos. Embryos and larvae were put on poly-L-lysine-coated slides and fixed by adding 10μl of 5% paraformaldehyde to embryos and larvae that were in 5 μl of water, incubated for 30 min in a wet chamber at room temperature and frozen on a chilled aluminum block for 5 min. After freeze cracking, the samples were placed in cold methanol (−20 °C) and cold acetone (−20 °C) for ten minutes. Rehydratation was done in a series of rehydratation buffers in ethanol (10 min in 90% cold ethanol, 60% cold ethanol, 30% ethanol at room temperature, and 1 h in TTBS — Tris-Tween-buffered saline). The NMY-2 antibody () was then applied in a 1:50 dilution and the slides kept in a wet chamber overnight at 4 °C. The next day the slides were washed 3× in TTBS and a secondary antibody (goat anti rabbit IgG AF 488 antibody, goat anti mouse IgM AF 488 antibody — diluted 1:100) was added. The slides were incubated for 2 h at room temperature, washed 3× in TTBS and mounted in 10 μl of mounting medium.

3. Results

3.1. Yeast two hybrid screens identified transcription and translation regulating proteins as well as structural proteins and ribosomal proteins as BIR-1 and SKP-1 interactors

Previous suggestions of functional connections between SKP-1 and BIR-1 [15,17,25], led us to determine if these two proteins may interact on the protein level, directly or indirectly. We screened for their interacting proteins using yeast two-hybrid screens for both *skp-1* and *bir-1* in a commercially available *C. elegans* library.

The search for SKP-1 interacting proteins identified proteins involved in translation: translation initiation factors 2B and 4A, polyadenylate binding protein PAB-1, ribosomal protein RPL-5 and RPL-11, and transcription cofactor TAC-1, NHR-92 and Myosin Heavy Chain protein (Table 1).

BIR-1 interaction studies yielded NHR-6, acid ribosomal protein RLA-0 and PAL-1, and two Y-box containing cold shock proteins, CEY-1 and CEY-2, that are homologues of vertebrate proteins that regulate gene expression on the level of transcription as well as mRNA in the cytoplasm (Table 2). Neither screen identified a direct interaction between SKP-1 and BIR-1. We also directly tested their potential interaction using the yeast two-hybrid system by cloning BIR-1 in one vector and SKP-1 in the other vector. This system did not

Table 1 – Proteins identified as SKP-1 interactors in a yeast two-hybrid screen.

No	Sequence	Gene/protein type
1	F11A3.2/C50F4, NM_073051.1	eIF-2B
2	Y54E2A.3	TAC-1
3	F57B9.6a	INF-1 (orthologous to mammalian eIF-4A)
4	K02F2 (WBGene00001075)	DPY-14
5	W10G6.3	IFA-2 (intermediate filament)
6	4F2011, R08C7.3	H2A.F HTZ-1
7	Y45F10D.13, F56F12.1	SORB-1
8	F54C9.5	RPL-5
9	4K941, K04D7.1	RACK-1
10	C10G11.9, T27A3.4	Mitochondrial protein
11	Y106G6H	PAB-1
12	1E420, T03F1.7	Mitochondrial transcription factor B1
13	T22F3.4 gi|17563233|ref|NM_071607.1|	RPL-11.1
14	gi|671714|gb|L39894.1|CELCPR6A	CPR-6
15	3L413, T07A5	Myosin heavy chain
16	C05C10.4	PHO-11, Intestinal acid phosphatase protein 4 member 2K223
17	4C397, Y41D4B.8	NHR-92 (HNF4-like)
18	W02D7.3	Similar to Ankyrin and KH repeat

Table 2 – Proteins identified as BIR-1 interactors in a yeast two-hybrid screen.

No	Sequence	Gene/protein type
1	B0546.1	MAI-1
2	ZK1240.9	Ubiquitin ligase
3	C48D5.1	NHR-6
4	T10E10.2	COL-167
5	F32B6.2	MCCC-1
6	C38D4.6	PAL-1
7	F46F11.2	CEY-2
8	D2096.3	Glycoside dehydrogenase
9	F33A8.3	CEY-1
10	F25H2.10	RLA-0

Table 3 – Proteins detected by MS in fractions with chromatographically altered pattern in two-dimensional comparative chromatography.

Protein	Gene	GO (WormBase WS243)
A. Proteins identified only in BIR-1 hyperinduction fractions		
40S ribosomal protein S3	*rps-3*	Apoptotic process, lifespan, embryo dev., molting, larval dev., reproduction, translation
Putative sideroflexin-like protein AH6.2	AH6.2	Cation transport
ATP synthase subunit alpha, mitochondrial precursor	H28O16.1	ATP binding, rotational mech.
60S ribosomal protein L5	*rpl-5*	Body morphogen., embryo and larval dev., reproduction, translation, (apoptosis in vertebrates)
Myosin-4 (UNC-54)	*unc-54*	Morphogen., locomotion, myosin assembly
Nuclear anchorage Protein1	*anc-1*	Cytoskeleton organization, pronuclear migration
B. Proteins identified only in wild type (N2) fractions		
Probable electron transfer flavoprotein subunit	F27D4.1	Embryo and larval dev., mitochondrial
Hit-like protein TAG-202	*tag-202*	Catalytic (tumor suppressor in vertebrates)
Triosephosphate isomerase	*tpi-1*	Catalytic
Uncharacterized protein B0303.3	B0303.3	Metabolic, mitochondrion
Probable 26S protease regulatory subunit S10	*rpt-4*	Morphogenesis, proteasome regulation
Probable ornithine aminotransferase, mitochondrial protein	C16A3.10	Catalytic, transaminase activity
Probable malate dehydrogenase mitochondrial protein	*mdh-1*	Catalytic
Probable prefoldin subunit 5	R151.9 *pfd-5*	Embryo dev., pronuclear migration, protein folding, locomotion
Superoxide dismutase [Cu–Zn]	*sod-1*	Metabolic, germ cell dev., striated muscle myosin thick filament assembly
Heat-shock protein Hsp-12.2	*hsp-12.2*	Reproduction, hsp binding
Glyceraldehyde-3-phosphate dehydrogenase 2	*gpd-2*	Metabolic, development
C. Proteins identified differentially in both N2 and BIR-1 hyperinduction fractions		
NHP2/L7aE family protein YEL026W homologue	M28.5	Morphogenesis, development
Protein UNC-87, a calponin-related protein	*unc-87*	Actin bundle assembly, morphogenesis
Transthyretin-like protein T07C4.5 precursor	T07C4.5	Extracellular (enriched in muscle)
Tropomyosin isoforms a/b/d/f + c/e	*lev-11*	Morphogenesis, development, cytokinesis, molting, negative regulation of actin filament depolymerization
Myosin, essential light chain	*mlc-3*	Locomotion, oviposition
Elongation factor 1-alpha	*eft-3*	Apoptosis, development, growth, translational elongation
Fructose-bisphosphate aldolase 2	F01F1.12	Catalytic, embryo dev., reproduction
40S ribosomal protein S8	*rps-8*	Apoptosis, development, translation
40S ribosomal protein S21	*rps-21*	Molting, development, translation

show direct interaction between BIR-1 and SKP-1 either (not shown).

3.2. *Short-time forced overproduction of BIR-1 induces chromatographic alterations of proteins functionally linked to SKP-1 interactors*

Since our yeast-two hybrid experiments indicated that SKP-1 and BIR-1 may influence gene expression through shared pathways, but did not show a direct interaction, we attempted to visualize the effect of BIR-1 short-time forced over expression on the whole proteome using a proteome differential display of *C. elegans* synchronized L1 larvae. We hypothesized that this experimental setting may help us visualize the involvement of BIR-1 on proteins functionally shared with SKP-1, which cannot be easily targeted in other ways.

To determine the time course of maximal expression, heat shock induced BIR-1 was monitored at the mRNA level by quantitative RT-PCR. This showed that at the time of harvesting larvae for the proteome study, the mRNA level of BIR-1

Fig. 1 – Two dimensional comparative chromatography of complete proteomes of control and BIR-1 overexpressing L1 Larvae. Panel A — first dimensional separation of protein lysates from wild type (N2) (red line) and *bir-1* overexpression samples (green line). Comparative analysis shows significant changes in the whole pI spectrum. The pH changes from pH 8.5 to pH 4 (arrowheads). In the last third of the chromatogram, proteins are eluted at pH 4 with an increasing concentration of NaCl to elute acidic proteins. Panel B — second dimension separation. A representative chromatogram of second dimension separation (fraction A2). The arrows indicate elevated absorbance (A_{214}) indicating higher protein content in the eluate in BIR-1 overexpressing larvae (green line) during the particular chromatographic time (arrows). Panel C — graphical representation of the differential proteome using the DeltaVue computer program. The protein content in particular chromatographic fractions is indicated in a gel-like pattern by red (for control proteome) and green colors (proteome of BIR-1 overexpressing larvae). The protein difference is indicated by the intensity of the color. Proteins constituting ninety eight paired fractions that showed a prominent difference in protein content were used for analysis by mass spectrometry. The arrow in panel C indicates a fraction containing elevated amount of protein in BIR-1 overexpressing larvae corresponding to the peak visible in the second dimension chromatogram (panel B, left arrow). There are clearly visible dramatic differences in the differential display of both proteomes across the pH spectrum.

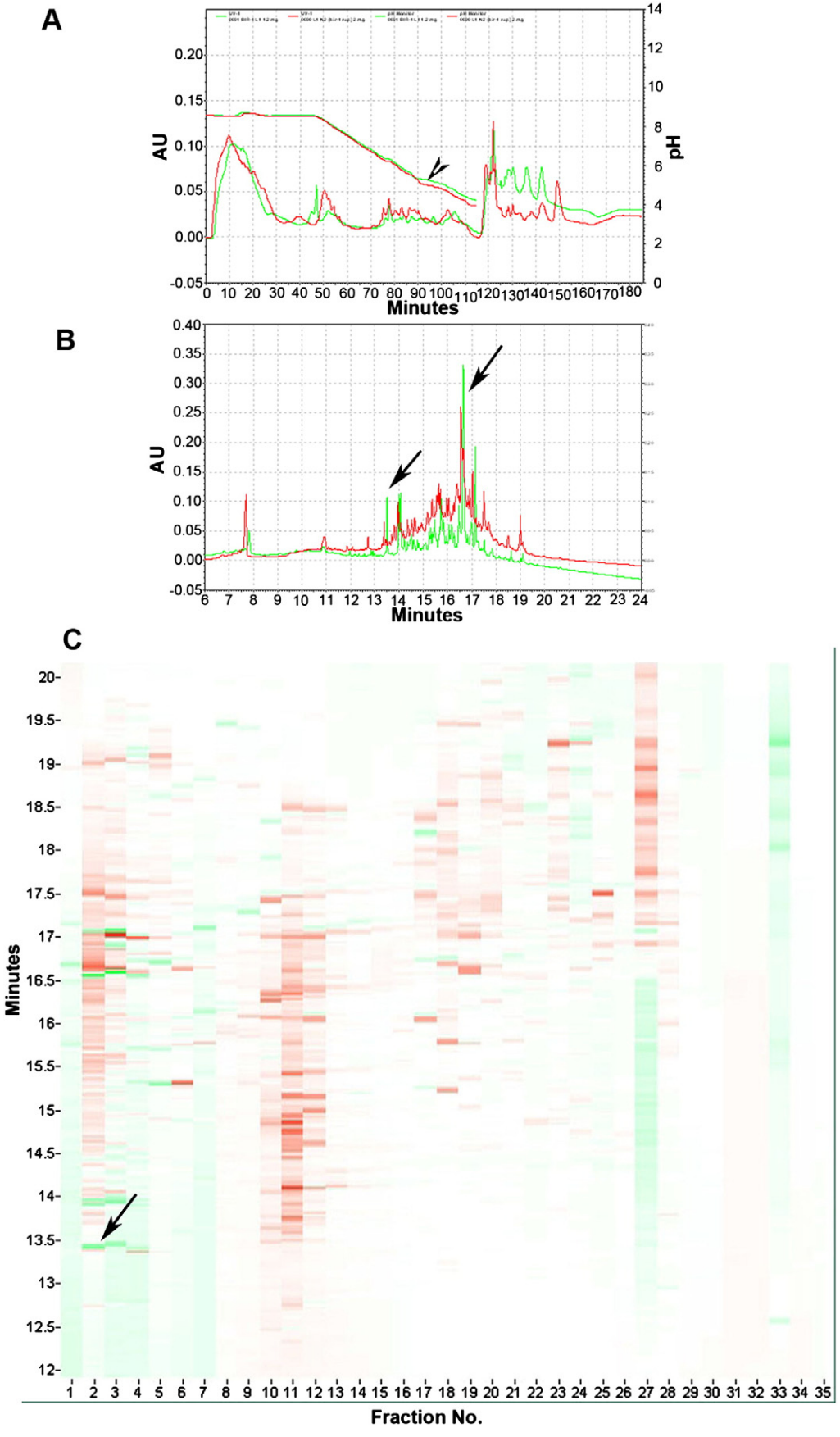
A
AU
pH
Minutes
B
AU
Minutes
C
Minutes
Fraction No.

was approximately 20 times higher than in control animals. Experiments for detection of a possible adverse effect of forced expression of BIR-1 were also conducted. As in previous experiments, we did not observe any developmental phenotype or defects of mitoses in larvae expressing increased levels of *bir-1* even after prolonged exposures.

For the comparative near-whole proteome analysis, we used the Proteome Lab Protein fractionation system (Beckman-Coulter, Brea, CA, USA). Protein lysates from synchronized *C. elegans* larvae with heat shock induced BIR-1 and wild type controls were obtained and small proteins eliminated together with salts on PD10 columns (with the fractionation range Mr 5000) thus eliminating proteins smaller than approximately 45 AA. The complete proteomes were separated using pH/NaCl gradient in the first dimension and stored in 40 fractions for each proteome (Supplementary Table S1).

Chromatographic profiles obtained from these samples clearly differed in specific regions between BIR-1 overproduction and the control proteomes (Fig. 1 A). In the second dimension chromatographic analysis (protein separation by hydrophobicity) approximately 1200 fractions were obtained from each control and experimental proteome. As shown on a representative chromatogram, BIR-1 hyperinduction leads to specific increases and decreases of protein content in fractions collected during the chromatographic elution. Differential display of the control and BIR-1 induction proteomes was obtained using DeltaVue software provided by the manufacturer (Fig. 2 B). The two dimensional comparative chromatography showed, to our surprise, that short time-forced expression of *bir-1* led to complex proteome changes in approximately 100 chromatographic fractions. 98 fractions were selected for further analysis by mass spectrometry. Spectrum analysis by SEQUEST™ software against the SwissProt database identified numerous *C. elegans* proteins together with proteins assigned to other species including bacteria and vertebrates. Filtering against confidence criteria (score, number of peptides) and selecting only *C. elegans* proteins yielded 24 proteins that were detected in 8 fractions (Supplementary Table S2). Seventeen proteins showed clear differences between larvae expressing large levels of BIR-1 and controls (Table 3A and B). These proteins were detected by mass spectrometry with high confidence only in fractions from BIR-1 overexpressing larvae (Table 3A) or only in the paired fraction from control larvae (Table 3B and Supplementary Tables S2 to S9). Nine proteins were detected with high confidence in both paired fractions (Table 3 C) including myosine and tropomyosin in acidic fraction (fraction 27) and elongation factor EF1 alpha. Interestingly, these proteins are likely to be shifted in BIR-1 overproducing larvae to more acidic fractions (Fig. 1 C, first dimension fraction No. 33) (but were not confirmed by mass spectrometry). These proteins were considered as candidate differential proteins. Their likely shift to more acidic fractions (especially fraction No. 33) can be seen in the chromatograms shown in Supplementary Figures S1 to S9. In addition to proteins with high confidence score, mass spectrometry detected many proteins with lower confidence scores. These proteins were not included in further analyses.

Gene ontology analysis of proteins identified as differentially expressed in BIR-1 overexpressing larvae compared to control N2 larvae using David Ontology Tool indicated BIR-1 involvement in the regulation of growth, embryonic development, molting cycle and cuticle formation, larval morphogenesis, locomotion, larval development, translational elongation and translation and gamete generation.

The set of proteins clearly affected by BIR-1 induction included ribosomal proteins RPS-3 and RPL-5 and myosin. These proteins were further analyzed functionally for a possible connection with BIR-1 and SKP-1 together with interacting proteins identified by yeast two-hybrid screens which were indicating shared involvement of BIR-1 and SKP-1 in the ribosomal stress pathway, in apoptosis and in the regulation of cytoskeleton during mitosis.

3.3. *Analyses targeted at selected proteins validate regulatory roles of SKP-1 and BIR-1 proteome interactions*

The protein interactions identified in yeast two hybrid screens indicated that SKP-1 and BIR-1 may be part of functionally linked protein complexes. The variability and expected cellular localizations of identified protein interactors led us to conclude that the interactions are likely to occur in separate cellular compartments and at specific conditions. We have chosen selected proteins for additional studies for validation of proteomic data.

Because the yeast two-hybrid screens demonstrated that TAC-1 interacts with SKP-1, we wondered if these two proteins are related functionally. TAC-1, a transforming coiled coil protein, is a known cofactor of nuclear receptors and is indispensable for normal centrosomal functions, centrosome migration and mitosis [26]. Therefore, we studied the effects of SKP-1 inhibition on mitosis in detail (Fig. 2) specifically assaying for the characteristic TAC-1 reduction-of-function phenotypes in centrosome migration during G2 phase. Staining of SKP-1 inhibited embryos with an antibody against SPD-2 [24] showed that SKP-1 inhibition led to serious defects of mitoses including endomitoses and defects of centrosome migration in the G2 phase (Fig. 2 F), similar to those previously shown following TAC-1 inhibition [27].

A protein category that is clearly represented in our yeast two-hybrid screen for SKP-1 interactome, as well as in BIR-1 hyperinduction, is ribosomal proteins. Interestingly, three specific proteins found in our study are ribosomal proteins involved in the ribosomal stress pathway [28–31]. We have therefore searched if the proteins that were identified in our experiments may interact with BIR-1 and SKP-1 in a GST fusion system. We prepared GST-fusion proteins and precipitated in vitro transcribed ribosomal proteins labeled with ^{35}S-methionine. Both GST-BIR-1 and GST-SKP-1, but not GST alone, showed binding to RPS-3 and RPL-5 (Fig. 3).

Since three myosin-related proteins were identified as protein species with an altered chromatographic pattern in BIR-1 hyperinduced larvae compared to controls, we searched if BIR-1 overproduction alters the immunocytochemical pattern of non-muscle myosin. As shown in Fig. 4 B, forced expression of *bir-1* leads to more prominent staining of NMY-2 at the cellular peripheries.

We also searched if the short exposure of *C. elegans* larvae to high levels of BIR-1 may affect organization of intermediate filaments in epidermis using a monoclonal antibody MH27 that specifically recognizes the MH-27 protein, which is similar to human trichohyalin, and is likely to be involved in organizing intermediate filaments in the hypodermis. As shown in Fig. 4 D, larvae that developed in the presence of

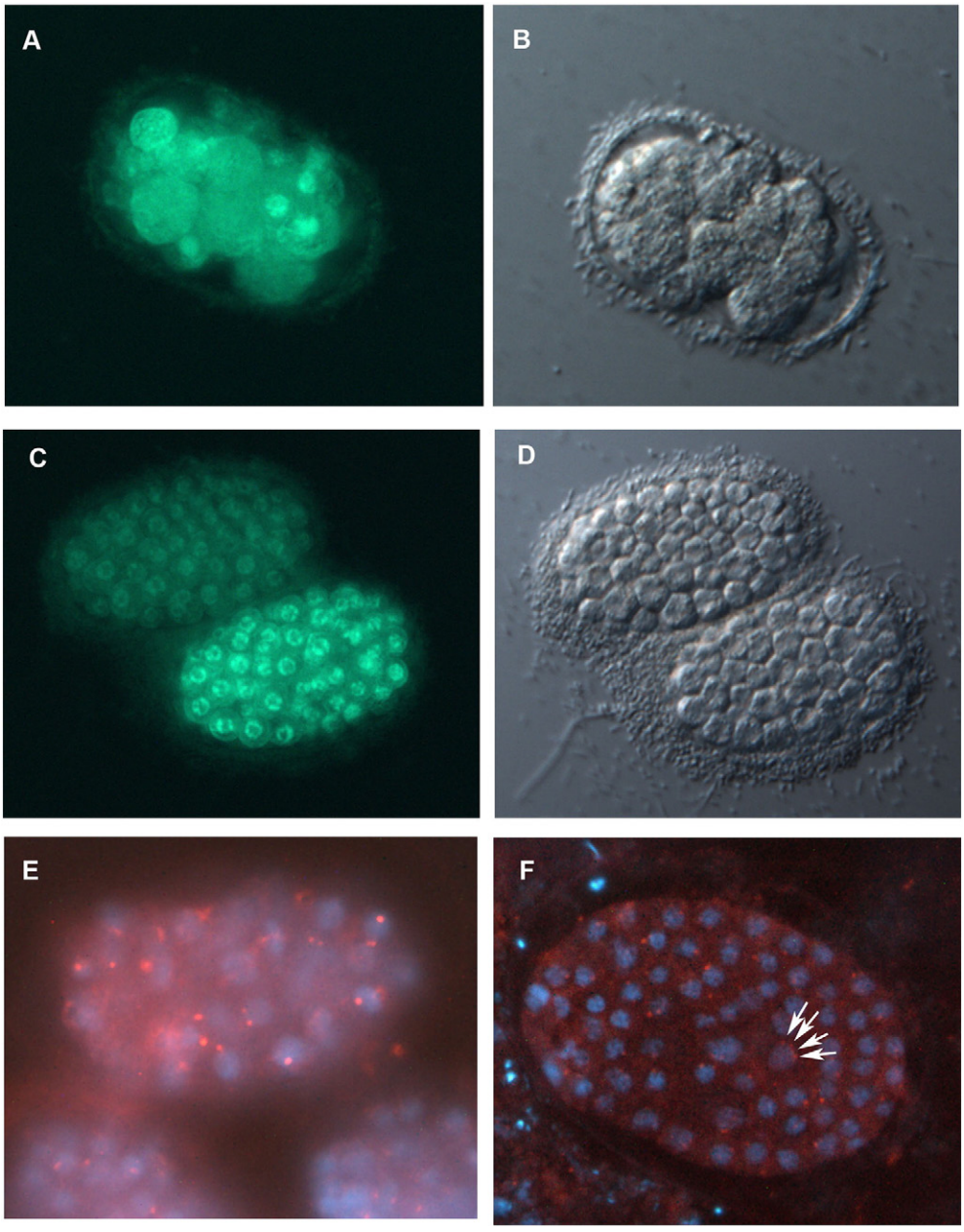

Fig. 2 – Inhibition of SKP-1 induces cell division arrest and endomitoses. Panels A and C show Histone H2::GFP expressing embryos. B and D are corresponding views in Nomarski optics. A and B show mitotic defects of *skp-1* RNAi embryos. The nuclei lost their regular architecture and the embryo arrested at approximately the 20 cell stage of development. Panel E shows a control embryo stained for DAPI and centrosomes. An embryo treated with *skp-1* RNAi (panel F) stained in the same way is arrested in development and contains cells that underwent endomitotic divisions with twice duplicated centrosomes with defective migration (arrows).

high expression of *bir-1* had higher levels of MH-27 localized at cellular borders of seam cells compared to controls. This supports the relevance of cytoskeletal and motor proteins detected as targets of BIR-1 at the protein level.

4. Discussion

In this study, we searched for possible links between SKP-1 and BIR-1. These proteins are coexpressed from one operon and their loss of function phenotypes was shown to be linked to the regulation of gene expression and development [15,17]. Both SKIP and BIR-1/Survivin are evolutionarily old highly conserved proteins that may be expected to be important for fundamental regulatory events. In this work, we searched for immediate protein functions that may transmit their cellular roles. We searched for interactors of SKP-1 and BIR-1 and identified proteins with overlapping and complementary functions as SKP-1 and BIR-1 interactors in yeast two hybrid screens. However, we did not observe a direct interaction

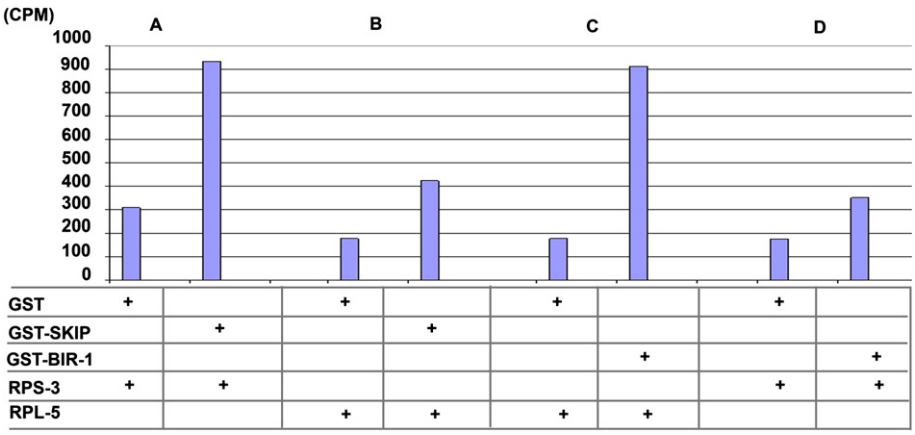

Fig. 3 – SKP-1 and BIR-1 interact with RPS-3 and RPL-5. Panels A to D show interactions of SKP-1 (panels A and B) with RPS-3 and RPL-5 (panels A and B, respectively) and interactions of BIR-1 with RPL5 and RPS-3 (panels C and D).

between SKP-1 and BIR-1. The character of processes in which SKP-1 and BIR-1 are involved, the regulation of gene expression and cell division makes their analysis difficult. Mitosis itself has profound effect on the proteome and this effect has to be distinguished from proteome states caused by specific developmental or metabolic regulators. *C. elegans* is a suitable system for combined functional and proteomic studies focused at proteins that function in interphase as well as in mitosis. In *C. elegans*, cell divisions occur in embryonic and larval stages in a precisely timed way and it is possible to obtain synchronized larval cultures that contain almost exclusively non-dividing cells. During larval stages (L1, L2) only a few cells divide and the growing gonad is small and does not affect significantly the complete proteome. This opens a wealth of possibilities for experimental functional analyses for proteins with multiple roles.

In our case, we studied the effect of short time BIR-1 hyperinduction on the *C. elegans* proteome in non-dividing cells. This approach identified several proteins found by yeast two-hybrid screens as SKP-1 and BIR-1 interactors also as targets of BIR-1 hyperinduction on the proteomic level. The wide range of proteins identified as SKP-1 and BIR-1 interactors by both approaches included cytoskeletal and motor proteins, ribosomal proteins known to be active in the ribosomal stress pathway and transcription and translation regulating proteins. The BIR-1 hyperinduction had a profound effect on the composition of the whole proteome in non-dividing cells. This indicated that BIR-1 hyperinduction may influence a wide spectrum of target proteins and/or regulates proteins that affect other proteins. Some proteins found by our screens fulfill these criteria: protein involved in the proteasome pathway, enzymes, and transcription and translation regulators.

Selected proteins that were studied functionally supported the concept that incorporation of BIR-1 and SKP-1 in cellular mechanistic events may be linked to their regulatory roles in major cellular events: cell cycle progression and mitosis, ribosomal stress, (and apoptosis) and gene expression.

Some connections were expected from known functions of BIR-1 or its vertebrate homologue Survivin. The connection between BIR-1 and non-muscle myosin is in agreement with the Survivin role in cytokinesis revealed by a separation-of-function mutant [32].

Identification of ribosomal proteins as both SKP-1 and BIR-1 interactors and targets of BIR-1 hyperinduction was unexpected but it further supports the functional connections between these two factors. The direct binding of SKP-1 and BIR-1 to RPS-3 and RPL-5 was confirmed by pull-down experiments. The physical interaction between SKP-1 and BIR-1 with ribosomal proteins that are known to participate in the ribosomal stress pathway opens a possibility that both SKP-1 and BIR-1 may be or their evolutionary ancestors were involved in ribosomal stress and apoptosis. Although *C. elegans* doesn't have a known MDM2 ortholog, it is likely that a protein that is still not recognized in the *C. elegans* genome supports this function. MDM2-p53 is a very ancient regulatory pathway that is already functional in a basal Metazoan — *Trichoplax adhaerens* [33,34]. MDM2 can reversely bind ribosomal proteins RPS3 [31], RPL5 [29,35,36], RPL11 [28,30,37,38], and RPS28 [39]. Additional proteins were shown to participate in the regulation of p53 pathway, including RPL37, RPS15, and RPS20 [39]. Various ribosomal proteins in the p53 pathway may function through multiple mechanisms, as was recently shown for ribosomal protein S26 [40]. SKP-1 and BIR-1 are thus likely to be functionally linked on multiple levels in the regulation of apoptosis, stress pathways and gene expression. Keeping with this, SKP-1 counteracts p53-regulated apoptosis through regulation of p21Cip1 mRNA splicing [41]. It seems likely, that SKP-1 and BIR-1's role in the regulation of apoptosis through interaction with ribosomal proteins may be more ancient than the role of Survivin in inhibition of apoptosis through the direct binding and inactivation of caspases. In *C. elegans*, BIR-1 doesn't regulate apoptosis through inactivation of caspases but its role in apoptosis induced by ribosomal stress was not yet tested. This Survivin's capacity may have evolved later in evolution on the basis of BIR/Survivin ability to physically interact with variable proteins.

There are additional lines of evidence indicating that SKP-1 and BIR-1 may be functionally linked at the proteome level. BIR-1 is a regulator of microtubule attachment to chromosomes in anaphase and progression of mitosis. TAC-1 that

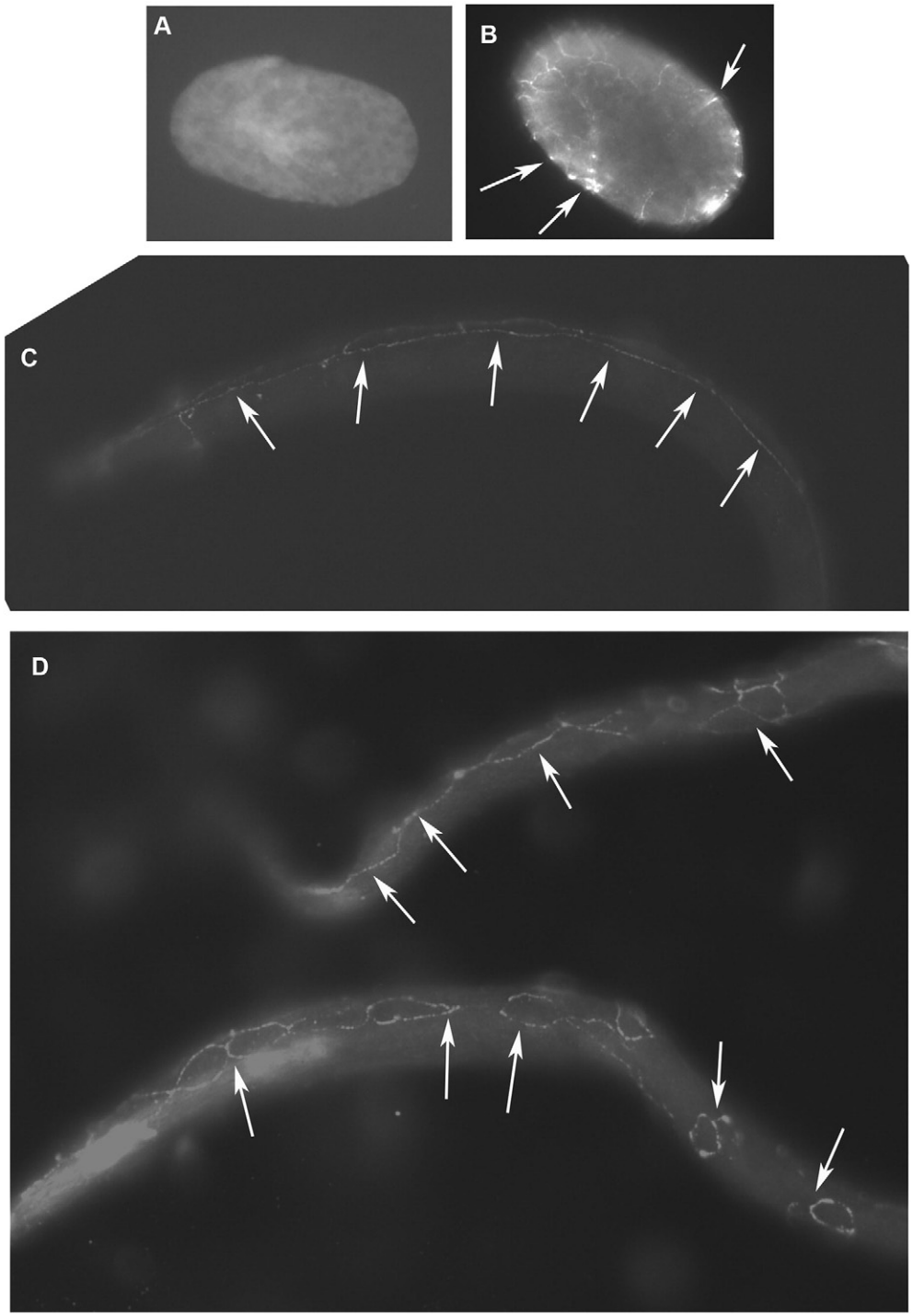

Fig. 4 – The effect of short term overexpression of *bir*-1 on non-muscle myosin localization in *C. elegans* embryos and development of seam cells. Panels A and B show *C. elegans* embryos stained for NMY-2. A) Control wild type (N2) embryo (containing control transgene consisting of empty vector), B) Embryo overexpressing *bir*-1 from a transgene regulated by heat shock promoter. Arrows indicate accumulation of NMY-2 at the cell borders. Panels C and D show L1 larvae stained for MH27 antigen. Panel C shows a control larva with regularly developed seam cells forming a ribbon of rectangular cells along the length and side of the animal. Panel D shows a L1 larva that developed from embryos affected by short term *bir*-1 overexpression. Arrows indicate seam cells that are bigger than in wild type controls, not properly connected to each other, and that often have an irregular shape.

was found as SKP-1 interactor has a critical role in mitosis specifically in the relocation of ZYG-9 to centrosomes. TAC-1 is found localized on centrosomes as well as in the nucleus where it plays critical roles in gene expression regulation. Interestingly, SKP-1 inhibition results in the same cellular event — G2 arrest and failure of centrosome migration as is known for TAC-1 [26]. A possibility of direct centrosomal localization and function of SKIP is keeping with the centrosomal localization and mitotic function of SKI [42,43], a protein which is interacting physically and functionally with SKIP [44].

Taken together, the protein interactions of SKP-1 and BIR-1 meet in major cellular events: cell division, ribosomal stress and apoptosis and gene expression.

Our results suggest that BIR-1 and SKP-1 are part of a larger network that is likely to participate not only on the same mechanistic events but that this network also has a potential to connect proteome signals with the regulation of gene expression on multiple levels. Several lines of evidence indicate that this network is real and functionally important. For example, SKIP is known to be a multifunctional protein involved in the regulation of transcription and is a co-activator for nuclear receptors [5,6,8]. SKIP also interacts with nuclear receptor co-repressor SMRT and functions in the Notch pathway through binding of Notch IC that is required for Notch biological activity [9]. SKIP also directly binds the retinoblastoma tumor suppressor protein pRb and, in co-operation with Ski, overcomes the G1 arrest induced by pRb [45]. SKIP is also involved in regulation of splicing [12,13,46,47]. Thus, SKIP has a well-documented role in the regulation of transcription and cell cycle.

It may be hypothesized that the pleiotropic protein interactions that we have identified for SKP-1 and BIR-1 are part of a proteome regulatory network with the capacity to project proteomic states towards gene expression regulation. Our data further link functionally SKP-1 and BIR-1. Both proteins bind proteins of the ribosomal stress pathway and possibly other stress pathways. SKIP was shown to be affecting stress related genes in plants. In rice and in *Arabidopsis*, it regulates stress related genes [48,49]. The ribosomal stress pathway thus may represent a special case of the cytoplasmic proteomic signals towards gene expression. If such proteomic signaling would be proved as a more general mechanism by which proteome composition projects directly towards gene expression, it may be considered as a proteome code. Such regulatory loops should include proteins that are localized in specific cellular structures and when liberated or synthesized in excess of cellular needs assume their additional regulatory roles. In fact, such inhibition of gene expression was shown to be the autoregulatory mechanism for RPL-12, which was shown to affect its own splicing most likely through a sensor affecting transcription [50]. SKP-1 and/or BIR-1 may be the sensor(s) in ribosomal protein transcription and in the ribosomal stress pathway.

5. Conclusion

Our proteomic analyses further support the functional links between SKP-1 and BIR-1 with connected and overlapping roles in the ribosomal stress pathway and transcriptional regulation. It seems likely, that SKP-1 and BIR-1/Survivin are involved in the ribosomal stress pathway and are possibly components of complexes connecting cellular needs with the regulation of gene expression at the level of transcription and translation.

Supplementary data to this article can be found online at http://dx.doi.org/10.1016/j.jprot.2014.07.023.

Transparency document

The Transparency document associated with this article can be found, in the online version.

Acknowledgments

DK, MK Jr. (Markéta Kostrouchová), PY, AC, JPN, PN, VK, MK, and ZK performed the experiments, participated on planning of experiments and wrote the manuscript; DK, MK Jr., PY, AC, JPN, VK, MK, and ZK were supported by grant PRVOUK-P27/LF1/1 from the Charles University in Prague, DK, MK Jr., PY, AC, JPN were supported by SVV 266505/2013 and SVV 260023/2014, PN was supported by the Institutional Research Concept RVO 61388971 (P.N.); DK, MK Jr., PY, AC, JPN, PN, VK, MK, and ZK are supported by the European Regional Development Fund "BIOCEV — Biotechnology and Biomedicine Centre of the Academy of Sciences and Charles University in Vestec" (CZ.1.05/1.1.00/02.0109); ZK, MK, MK Jr, and DK were supported by the Intramural Research Program of the National Institute of Diabetes and Digestive and Kidney Diseases (NIDDK) of the National Institutes of Health, USA. ZK and MK contributed with personal funds to this work. The authors are very grateful to Dr. Michael W. Krause, NIDDK, NIH, Bethesda for his support and help during all stages of the work connected with this project and preparation of the manuscript. The authors thank WormBase for bioinformatic support. No additional external funding was received for this study. The funders had no role in the study design, data collection and analysis, decision to publish, or preparation of the manuscript.

REFERENCES

[1] Saumweber H, Frasch M, Korge G. Two puff-specific proteins bind within the 2.5 kb upstream region of the *Drosophila melanogaster* Sgs-4 gene. Chromosoma 1990; 99:52–60.
[2] Wieland C, Mann S, von Besser H, Saumweber H. The *Drosophila* nuclear protein Bx42, which is found in many puffs on polytene chromosomes, is highly charged. Chromosoma 1992;101:517–25.
[3] Folk P, Puta F, Krpejsova L, Blahuskova A, Markos A, Rabino M, et al. The homolog of chromatin binding protein Bx42 identified in Dictyostelium. Gene 1996;181:229–31.
[4] Martinkova K, Lebduska P, Skruzny M, Folk P, Puta F. Functional mapping of *Saccharomyces cerevisiae* Prp45 identifies the SNW domain as essential for viability. J Biochem 2002;132:557–63.
[5] Baudino TA, Kraichely DM, Jefcoat Jr SC, Winchester SK, Partridge NC, MacDonald PN. Isolation and characterization

of a novel coactivator protein, NCoA-62, involved in vitamin D-mediated transcription. J Biol Chem 1998;273:16434–41.
[6] Barry JB, Leong GM, Church WB, Issa LL, Eisman JA, Gardiner EM. Interactions of SKIP/NCoA-62, TFIIB, and retinoid X receptor with vitamin D receptor helix H10 residues. J Biol Chem 2003;278:8224–8.
[7] Fantappie MR, de Oliveira FM Bastos, de Moraes Maciel R, Rumjanek FD, Wu W, Loverde PT. Cloning of SmNCoA-62, a novel nuclear receptor co-activator from *Schistosoma mansoni*: assembly of a complex with a SmRXR1/SmNR1 heterodimer, SmGCN5 and SmCBP1. Int J Parasitol 2008;38:1133–47.
[8] Abankwa D, Millard SM, Martel N, Choong CS, Yang M, Butler LM, et al. Ski-interacting protein (SKIP) interacts with androgen receptor in the nucleus and modulates androgen-dependent transcription. BMC Biochem 2013;14:10.
[9] Zhou S, Fujimuro M, Hsieh JJ, Chen L, Miyamoto A, Weinmaster G, et al. SKIP, a CBF1-associated protein, interacts with the ankyrin repeat domain of NotchIC To facilitate NotchIC function. Mol Cell Biol 2000;20:2400–10.
[10] Wang Y, Fu Y, Gao L, Zhu G, Liang J, Gao C, et al. Xenopus skip modulates Wnt/beta-catenin signaling and functions in neural crest induction. J Biol Chem 2010;285:10890–901.
[11] Leong GM, Subramaniam N, Figueroa J, Flanagan JL, Hayman MJ, Eisman JA, et al. Ski-interacting protein interacts with Smad proteins to augment transforming growth factor-beta-dependent transcription. J Biol Chem 2001; 276:18243–8.
[12] Zhang C, Dowd DR, Staal A, Gu C, Lian JB, van Wijnen AJ, et al. Nuclear coactivator-62 kDa/Ski-interacting protein is a nuclear matrix-associated coactivator that may couple vitamin D receptor-mediated transcription and RNA splicing. J Biol Chem 2003;278:35325–36.
[13] Wang X, Wu F, Xie Q, Wang H, Wang Y, Yue Y, et al. SKIP is a component of the spliceosome linking alternative splicing and the circadian clock in *Arabidopsis*. Plant Cell 2012; 24:3278–95.
[14] Leong GM, Subramaniam N, Issa LL, Barry JB, Kino T, Driggers PH, et al. Ski-interacting protein, a bifunctional nuclear receptor coregulator that interacts with N-CoR/SMRT and p300. Biochem Biophys Res Commun 2004;315:1070–6.
[15] Kostrouchova M, Housa D, Kostrouch Z, Saudek V, Rall JE. SKIP is an indispensable factor for *Caenorhabditis elegans* development. Proc Natl Acad Sci U S A 2002;99:9254–9.
[16] Li F, Ambrosini G, Chu EY, Plescia J, Tognin S, Marchisio PC, et al. Control of apoptosis and mitotic spindle checkpoint by survivin. Nature 1998;396:580–4.
[17] Kostrouchova M, Kostrouch Z, Saudek V, Piatigorsky J, Rall JE. BIR-1, a *Caenorhabditis elegans* homologue of Survivin, regulates transcription and development. Proc Natl Acad Sci U S A 2003;100:5240–5.
[18] Brenner S. The genetics of *Caenorhabditis elegans*. Genetics 1974;77:71–94.
[19] Tabb DL, McDonald WH, Yates III JR. DTASelect and Contrast: tools for assembling and comparing protein identifications from shotgun proteomics. J Proteome Res 2002;1:21–6.
[20] Pohludka M, Simeckova K, Vohanka J, Yilma P, Novak P, Krause MW, et al. Proteomic analysis uncovers a metabolic phenotype in *C. elegans* after nhr-40 reduction of function. Biochem Biophys Res Commun 2008;374:49–54.
[21] Altschul SF, Gish W, Miller W, Myers EW, Lipman DJ. Basic local alignment search tool. J Mol Biol 1990;215:403–10.
[22] Huang DW, Sherman BT, Lempicki RA. Systematic and integrative analysis of large gene lists using DAVID bioinformatics resources. Nat Protoc 2009;4:44–57.
[23] Huang DW, Sherman BT, Lempicki RA. Bioinformatics enrichment tools: paths toward the comprehensive functional analysis of large gene lists. Nucleic Acids Res 2009;37:1–13.
[24] Kemp CA, Kopish KR, Zipperlen P, Ahringer J, O'Connell KF. Centrosome maturation and duplication in *C. elegans* require the coiled-coil protein SPD-2. Dev Cell 2004;6:511–23.
[25] Liby P, Pohludka M, Vohanka J, Kostrouchova M, Kostrouch D, Rall JE, et al. BIR-1, the homologue of human Survivin, regulates expression of developmentally active collagen genes in *C. elegans*. Folia Biol (Praha) 2006;52:101–8.
[26] Bellanger JM, Carter JC, Phillips JB, Canard C, Bowerman B, Gonczy P. ZYG-9, TAC-1 and ZYG-8 together ensure correct microtubule function throughout the cell cycle of *C. elegans* embryos. J Cell Sci 2007;120:2963–73.
[27] Srayko M, Quintin S, Schwager A, Hyman AA. *Caenorhabditis elegans* TAC-1 and ZYG-9 form a complex that is essential for long astral and spindle microtubules. Curr Biol 2003;13:1506–11.
[28] Zhang Y, Wolf GW, Bhat K, Jin A, Allio T, Burkhart WA, et al. Ribosomal protein L11 negatively regulates oncoprotein MDM2 and mediates a p53-dependent ribosomal-stress checkpoint pathway. Mol Cell Biol 2003;23:8902–12.
[29] Horn HF, Vousden KH. Cooperation between the ribosomal proteins L5 and L11 in the p53 pathway. Oncogene 2008; 27:5774–84.
[30] Dai MS, Shi D, Jin Y, Sun XX, Zhang Y, Grossman SR, et al. Regulation of the MDM2-p53 pathway by ribosomal protein L11 involves a post-ubiquitination mechanism. J Biol Chem 2006;281:24304–13.
[31] Yadavilli S, Mayo LD, Higgins M, Lain S, Hegde V, Deutsch WA. Ribosomal protein S3: a multi-functional protein that interacts with both p53 and MDM2 through its KH domain. DNA Repair (Amst) 2009;8:1215–24.
[32] Szafer-Glusman E, Fuller MT, Giansanti MG. Role of Survivin in cytokinesis revealed by a separation-of-function allele. Mol Biol Cell 2011;22:3779–90.
[33] Lane DP, Cheok CF, Brown C, Madhumalar A, Ghadessy FJ, Verma C. Mdm2 and p53 are highly conserved from placozoans to man. Cell Cycle 2010;9:540–7.
[34] von der Chevallerie K, Rolfes S, Schierwater B. Inhibitors of the p53-Mdm2 interaction increase programmed cell death and produce abnormal phenotypes in the placozoon *Trichoplax adhaerens* (F.E. Schulze). Dev Genes Evol 2014;224:79–85.
[35] Dai MS, Lu H. Inhibition of MDM2-mediated p53 ubiquitination and degradation by ribosomal protein L5. J Biol Chem 2004;279:44475–82.
[36] Marechal V, Elenbaas B, Piette J, Nicolas JC, Levine AJ. The ribosomal L5 protein is associated with mdm-2 and mdm-2-p53 complexes. Mol Cell Biol 1994;14:7414–20.
[37] Lohrum MA, Ludwig RL, Kubbutat MH, Hanlon M, Vousden KH. Regulation of HDM2 activity by the ribosomal protein L11. Cancer Cell 2003;3:577–87.
[38] Morgado-Palacin L, Llanos S, Serrano M. Ribosomal stress induces L11- and p53-dependent apoptosis in mouse pluripotent stem cells. Cell Cycle 2012;11:503–10.
[39] Daftuar L, Zhu Y, Jacq X, Prives C. Ribosomal proteins RPL37, RPS15 and RPS20 regulate the Mdm2-p53-MdmX network. PLoS One 2013;8:e68667.
[40] Cui D, Li L, Lou H, Sun H, Ngai SM, Shao G, et al. The ribosomal protein S26 regulates p53 activity in response to DNA damage. Oncogene 2013;33:2225–35.
[41] Chen Y, Zhang L, Jones KA. SKIP counteracts p53-mediated apoptosis via selective regulation of p21Cip1 mRNA splicing. Genes Dev 2011;25:701–16.
[42] Mosquera J, Armisen R, Zhao H, Rojas DA, Maldonado E, Tapia JC, et al. Identification of Ski as a target for Aurora A kinase. Biochem Biophys Res Commun 2011;409:539–43.
[43] Marcelain K, Hayman MJ. The Ski oncoprotein is upregulated and localized at the centrosomes and mitotic spindle during mitosis. Oncogene 2005;24:4321–9.
[44] Prathapam T, Kuhne C, Hayman M, Banks L. Ski interacts with the evolutionarily conserved SNW domain of Skip. Nucleic Acids Res 2001;29:3469–76.

[45] Prathapam T, Kuhne C, Banks L. Skip interacts with the retinoblastoma tumor suppressor and inhibits its transcriptional repression activity. Nucleic Acids Res 2002; 30:5261–8.
[46] Figueroa JD, Hayman MJ. The human Ski-interacting protein functionally substitutes for the yeast PRP45 gene. Biochem Biophys Res Commun 2004;319:1105–9.
[47] Bres V, Gomes N, Pickle L, Jones KA. A human splicing factor, SKIP, associates with P-TEFb and enhances transcription elongation by HIV-1 Tat. Genes Dev 2005;19:1211–26.
[48] Hou X, Xie K, Yao J, Qi Z, Xiong L. A homolog of human ski-interacting protein in rice positively regulates cell viability and stress tolerance. Proc Natl Acad Sci U S A 2009;106:6410–5.
[49] Zhang Y, Zhao L, Li H, Gao Y, Li Y, Wu X, et al. GmGBP1, a homolog of human ski interacting protein in soybean, regulates flowering and stress tolerance in *Arabidopsis*. BMC Plant Biol 2013;13:21.
[50] Mitrovich QM, Anderson P. Unproductively spliced ribosomal protein mRNAs are natural targets of mRNA surveillance in *C. elegans*. Genes Dev 2000;14:2173–84.